Supporting Information

Inspired by Lubricin: A Tailored Cartilage–Armor with Durable Lubricity and Autophagy–activated Antioxidation for Targeted Therapy of Osteoarthritis

Peng Yu[a], Xu Peng[b], Hui Sun[a], Qiangwei Xin[a], Han Kang[c], Peng Wang[a], Yao Zhao[a], Xinyuan Xu[a], Guangwu Zhou[d], Jing Xie[a] and Jianshu Li[a,e]**

[a] College of Polymer Science and Engineering, State Key Laboratory of Polymer Materials Engineering, Med–X Center for Materials, Sichuan University, Chengdu 610065, P.R. China

[b] Experimental and Research Animal Institute, Sichuan University, Chengdu 610207, P.R. China

[c] Life Science Core Facilities, College of Life Sciences, Sichuan University, Chengdu 610065, P.R. China

[d] School of Aeronautics and Astronautics, Sichuan University, Chengdu 610207, P.R. China

[e] State Key Laboratory of Oral Diseases, West China Hospital of Stomatology, Sichuan University, Chengdu 610041, P.R. China

* Corresponding authors: Jianshu Li (fredca2005@163.com; jianshu_li@scu.edu.cn) and Jing Xie (xiej@scu.edu.cn)

Contents

S1. Experimental section

S1.1. Materials

Col II–target peptide (WYRGRL, purity > 98%) was obtained from Apeptide Co., Ltd (Shanghai, China). GGGGD peptide (purity > 95%) was provided by Shanghai Boti Biological Pharmaceutic Enterprise (Shanghai, China). Sulfobetaine methacrylate (SBMA), N–hydroxysuccinimide (NHS), triethylamine, nitrotetrazolium blue chloride (NBT), phenazine methosulfate (PMS), nicotinamide adenine dinucleotide disodium salt (NADH), 2–phenyl–4,4,5,5–tetramethylimidazoline–3–oxide–1–oxyl (PTIO), 1,1–diphenyl–2–picrylhydrazyl (DPPH) and 2,2'–azinobis (3–ethylbenzothiazoline–6–sulfonic acid ammonium salt) (ABTS) were bought form Aladdin (Shanghai, China). 4–cyano–4–(phenylcarbonothioylthio)pentanoic acid (CPAD), L–ascorbic acid, L–proline, sodium pyruvate and azodiisobutyronitrile (AIBN) were bought from J&K Scientific (Beijing, China). AIBN was further purified through recrystallization before use. Methacryloyl chloride was bought from TCI (Shanghai) Development Co., Ltd. (China). Trifluoroethanol (TFE) was obtained from Macklin (Shanghai, China). Dichloromethane (DCM), ethyl acetate (EA), hydrogen peroxide (H_2O_2) and n–hexane were bought from Xilong Chemical Co., Ltd (Shanghai, China). Bovine serum albumin, collagen type II (Col II), chondroitin sulfate (CS), hyaluronic acid (HA), collagenase II (Cls II), hyaluronidase (Hyase) and purified terephthalic acid (PTA) were obtained from Shanghai yuanye Bio–Technology Co., Ltd (China). Fluorescein isothiocyanate (FITC) and fluorescein diacetate (FDA) was provided by Sigma–Aldrich (USA). Fetal bovine serum (FBS) was obtained from Gibico (South Ameica). Penicillin–streptomycin and tyrisin were bought from HyClone (USA). Phosphate buffered saline (PBS) were provided by Gibico (USA). Cell counting kit (CCK–8) was obtained by MCE (USA). Propidium iodide (PI), 4’,6–diamidino–2–phenylindole (DAPI), lipopolysaccharides (LPS) from *Escherichia coli*, Enhanced BCA Protein Assay Kit, Periodic Acid–Schiff Staining Kit, Alcian Blue Staining Kit, Annexin V–FITC Apoptosis Detection Kit, Hoechst 33342., Hoechst 33358, 2', 7'–dichlorodihydrofluorescein diacetate (DCFH–DA), dihydroethidium (DHE), 3–Amino,4–aminomethyl–2’,7’–difluorescein, diacetate (DAF–FM), Griess reagent, Autophagy Staining Assay Kit with monodansylcadaverine (MDC)/PI (MDC/PI), Total Antioxidant Capacity Assay Kit with FRAP method (T–AOC Assay Kit), and Earle's Balanced Salt Solution (EBSS) were obtained from Beyotime (Shanghai, China). Dexamethasone, fluorescein isothiocyanate (FITC) and transforming growth factor–beta 3 (TGF–β3) were provided by Sigma–Aldrich (USA). TRITC Phalloidin and Hydrogen Peroxide (H_2O_2) Content Assay Kit were provided by Beijing Solarbio Science & Technology Co., Ltd. (Beijing, China). Insulin–transferrin–selenium (ITS) was provided by

ScienCell Research Laboratories (USA). Enzyme–linked immunosorbent assay (ELISA) kits of prostaglandin E2 (PGE–2), interleukin–6 (IL–6), tumor necrosis factor–alpha (TNF–α), collagen type II (Col II), and aggrecan (ACAN) were bought from Jiangsu Meimian Industrial Co., Ltd (Jiangsu, China). RAW 264.7 cell line and synovial mesenchymal stem cells (SMSCs) were obtained from Procell Life Science&Technology Co.,Ltd (Wuhan, China). Ultrapure water fabricated from the Milly–Q (Elix™ Essential 5, Merck Millipore, France) was used in all experiments. The chemical agents were used directly otherwise special statement.

S1.2. Synthesis of PSB–b–PColBP

S1.2.1. Synthesis of PSB–macroCTA (PSB) initiator

The PSBmacro–CTA was synthesized according to the literature report.[1] In brief, SBMA (5027.9 mg, 18 mmol, CPAD (50.3 mg, 0.18 mol) and AIBN (14.9 mg, 0.09 mol) were dissolved in TFE (5 mL). Oxygen (O_2) was removed by 3 cycles of "freezing–thawing", followed by nitrogen (N_2) purging for 15 to 30 min. The reaction was kept at 65 ^oC for 24 h. The product was purified by centrifugation in cold methanol for three times and subsequently dried under vacuum for 48 h.

S1.2.2. Synthesis of PSB–b–PNHS (PSN)

PSB (4331.0 mg), NHSMA (328.3 mg, 0.018 mol), and AIBN (10.1 mg, 0.06 mol) were dissolved in TFE (12 mL). Deoxygenation was performed through three cycles of "freezing–thawing", followed by N_2 purging for 15 to 30 min. After reacting at 65 ^oC for 24 h, the PSN were purified by centrifugation in cold methanol for three times and subsequently dried under vacuum for 48 h.

S1.2.3. Cartilage–targeting peptide conjugation

The collagen–binding peptide (ColBP, WYRGRL, 20 mg) was dissolved in phosphate buffered saline (PBS, pH = 8.0, 8 mL) at 40 ^oC. Separately, PSN (80 mg) was dissolved in ultrapure water (2 mL). The PSN solution was then added dropwise to the peptide solution. The mixture was allowed to react for 24 h. The PSB–*b*–PColBP (PSP) was purified through dialysis (MW 3,500 Da), followed by lyophilization to obtain the final product.

S1.3. Characterization of the zwitterionic polymers

The chemical compositions of PSB, PSN and PSP were characterized using nuclear magnetic resonance spectrometer (NMR, AV III HD 400 MHz, Bruker, German). X–ray photoelectron spectroscopy (XPS) was applied to investigate the element composition of the polymers. The

functional groups of zwitterionic polymers were analyzed using Fourier Transform infrared spectroscopy (FT–IR). The molecular weight distribution was determined using gel permeation chromatography (GPC). The peptide conjugation process was further analyzed using ultraviolet–visible (UV–vis) spectroscopy (TU1901, Presee, China), fluorescence spectrophotometry (RF–6000, SHIMADZU, Japan) and BCA Protein Assay Kit. Additionally, the peptide conformation was characterized using circular dichroism (CD) spectroscopy (JASCO-1500-150, Japan).

S1.4. Cartilage–targeting properties of PSP

S1.4.1. Molecular docking

The ColBP and PSP were subjected to molecular docking analysis. The protein structure of collagen type II (Col II) was obtained from PDB (https://www.Rcsb.org/). The molecular structures of ColBP, PSP, chondroitin sulfate (CS) and hyaluronic acid (HA) were drawn using ChemBio3D. AutoDockTools was adopted for docking analysis to calculate affinity energy. UCSF PyMol software was then applied to create the 3D images of the docking results, providing a visual representation of the molecular interactions.

S1.4.2. Specific targeting to Col II

Targeting to biomacromolecules of cartilage matrix: The WYRGRL hexapeptide was labelled by FITC as follows. First, the hexapeptide (10 mg) was dissolved in PBS (pH = 7.2–7.4, 5 mL), and FITC solution (200 μL) was added. The reaction mixture was kept in an ice bath with mild stirring for 24 h. Finally, dialysis (MWCO 1,000 Da) was performed for 3 d, followed by lyophilization to obtain the FITC–labeled hexapeptide. Col II, CS and HA solutions were prepared at a concentration of 1 mg/mL. Each solution was then incubated with FITC–labelled hexapeptide solution (1 mg/mL) at 37 °C in the dark for 24 h. After incubation, the mixtures were dialyzed against water (MWCO 2,000 Da) for 3 d to remove any unbond FITC–labeled hexapeptide. The fluorescence intensity of the resulting solutions was measured using a fluorescence spectrophotometry (RF–6000, SHIMADZU, Japan). The excitation wavelength was 488 nm, the emission wavelength range was 500~600 nm. Meanwhile, fluorescent images of three solutions under ultraviolet light irradiation at 365 nm were recorded.

Ex vivo targeting to cartilage: The femurs were collected from SD rats and subsequently incubated with FITC–labeled PSBG and PSP solutions for 24 h. The targeting efficiency was calculated according to formula (1).

$$TE\ (\%) = \frac{(FL_{original} - FL_{post-incubation})}{FL_{original}} \times 100 \quad (1)$$

where the $FL_{original}$ and $FL_{post–incubation}$ are the fluorescence intensity of the original polymer solution and post–incubated solutions with cartilage, respectively.

S1.5. Biolubrication test

S1.5.1 The anti–friction properties of PSP as biolubricant

The lubrication behavior of PSB and PSP (1 mg/mL) was analyzed using a universal materials tester (UMTtribolab, Bruker, Germany) with reciprocating sliding in ball–to–plate models. All tests were conducted using an Al_2O_3 sphere (d = 8 mm) as the ball and a polytetrafluoroethylene (PTFE) plate. The oscillation amplitude was 5 mm. The frequencies were 0.5, 1 and 1.5 Hz, respectively. The loading forces were 1, 2, and 3 N respectively. Each test lasted for 300 s. A polymer–free solution was also tested as a control for comparison.

S1.5.2. The targeted lubrication properties of PSP

A self–developed model has been utilized to the targeted lubrication of PSP, with PSBG used as a reference. Briefly, the femur specimens collected from SD rats were incubated with polymer solution (FITC–labelled PSBG or PSP, 1 mg/mL) at 37 °C for 24 h, and then washed by saline for several times. The modified femur specimens were embedded in dental resin materials and immobilized in a PTFE chamber. Meanwhile, PTFE slices have been bond to an objective table (20 g) bearing a weight of 1000 g. The rotational friction tests were carried out under saline solutions at frequencies of 0.5, 1.0 and 1.5 Hz, respectively. To investigate the durability of polymer–modified cartilage, similar test was conducted for 500 cycles. The cartilage surface, exposed to ultraviolent light at 365 nm, was recorded using a camera.

S1.6. Anti–oxidation evaluation of PSP

S1.6.1. ROS scavenging

As for H_2O_2 scavenging assay, H_2O_2 solution (1 mM) was incubated with polymers (PSB and PSP, 1 mg/mL) for 6 h at 37 °C. The remaining concentration of H_2O_2 was then determined using a Hydrogen Peroxide Assay Kit, following the manufacturer's instructions. Absorbance was recorded at approximately 415 using a UV–vis spectrophotometer. The scavenging ratio was calculated through formula (2):

$$H_2O_2\ scavenging\ ratio\ (\%) = \frac{A_0 - A_t}{A_0} \times 100 \quad (2)$$

where A_o refers to the absorbance of the original H_2O_2 solution and A_t refers to the absorbance of the remaining H_2O_2 concentration after incubating with PSP (or PSP) for 6 h.

In terms of the ·OH scavenging assay, polymers (1 mg/mL) were mixed with H_2O_2 solution (1 mM) supplemented with PTA (0.5 wt%). After incubation at 37 °C in the dark for 12 h, the fluorescence intensity of the mixed solution was recorded in the range of 400–600 nm using a fluorescence spectrophotometry with extraction wavelength at 315 nm.

The scavenging ratio of superoxide anion radicals (O·–2) was evaluated as follows: a working solution was prepared by mixing nicotinamide adenine dinucleotide disodium salt (NADH, 78 μM), phenazine methosulfate (PMS, 10 μM) and nitrotetrazolium blue chloride (NBT, 50 μM). PSP (or PSB) was then dissolved in the working solution to a concentration of 1 mg/mL and incubated for 0.5 h at 37 °C. The absorbance at 560 nm was measured using a UV–vis spectrophotometer. The scavenging ratio was calculated through formula (3):

$$O^{\cdot}{}_2^- \ scavenging\ ratio\ (\%) = \frac{A_0 - A_t}{A_0} \times 100 \quad (3)$$

where A_o is the absorbance of the working solution without polymer incubation, and A_t is the absorbance of the solution after polymer incubation.

In the PTIO test, the polymers were dissolved in PTIO solution (0.015 wt%) at a concentration of 1 mg/mL and incubated at 37 °C for 2 h. The absorbance at 557 nm was recorded using UV–vis spectrophotometer. The PTIO scavenging ratio was calculated through formula (4):

$$PTIO\ scavenging\ ratio\ (\%) = \frac{A_0 - A_t}{A_0} \times 100 \quad (4)$$

where A_o is the absorbance of the original PTIO solution, and A_t is the absorbance of the PTIO solution after incubation with PSP (or PSP).

The total superoxide dismutase (SOD)–like antioxidant activity was assessed using a Total Antioxidant Capacity Assay Kit with FRAP method (T–AOC Assay Kit). In brief, PSP (or PSB, 5 μL) solution was added to the FRAP working solution (180 μL) to achieve a final polymer concentration of 1 mg/mL. After incubating at 37 °C for 5 min, the optical density (OD) value at 593 nm was recorded using a microplate reader (SpectraMax® ABS Plus). The total antioxidant activity was calculated through formula (5):

$$Total\ anti-oxidation\ acticity = \frac{OD_c - OD_t}{OD_c} \quad (5)$$

where OD_c represents the absorbance of the $FeSO_4$ solution (1 mM) and OD_t represents the absorbance of polymer–incubated solution.

S1.6.2. RNS scavenging

For the DPPH assay, 3 mg of PSB or PSP were dissolved in DPPH solution (3 mL) and incubated in the dark at room temperature for 0.5 h. The absorbance at 517 nm was then recorded. The DPPH scavenging ratio was calculated according to formula (6):

$$DPPH\ scavenging\ ratio\ (\%) = \frac{A_0 - A_t}{A_0} \times 100 \quad (6)$$

where A_o and A_t refer to the absorbance of the DPPH solution without or with polymer incubation, respectively.

For the ABTS assay, a mixture containing ABTS (7.5 mM) and $(NH_4)_2S_2O_8$ (2.5 mM) was incubated in the dark at room temperature to generate ABTS cation radicals ($ABTS^+$). Then the $ABTS^+$ was diluted to to achieve an absorbance of approximately 0.7 at 734 nm. The polymers were dissolved in the $ABTS^+$ solution at a final concentration of 1 mg/mL and incubated in the dark for 0.5 h. The absorbance was recorded in the range of 550–800 nm. The scavenging ratio of $ABTS^+$ was calculated through formula (7):

$$ABTS^+\ scavenging\ ratio\ (\%) = \frac{A_0 - A_t}{A_0} \times 100 \quad (7)$$

where A_o and A_t refer to the absorbance of the $ABTS^+$ solution without or with polymer incubation, respectively.

S1.6.3. PSP suppresses intracellular oxidative stress

RAW264.7 cells, chondrocytes, BMSCs and SMSCs were seeded in 24–well plates. Once the cells were fully attached to the plates, lipopolysaccharide (LPS, 1 μg/mL) was utilized to induce an inflammation response. Following this, PSB and PSP were added to the culture medium at the concentration of 1 mg/mL. After 24 h of cultivation, the intracellular ·OH, O·–2, NO were detected using the dyes 2,7–dichlorodihydrofluorescein diacetate (DCFH–DA), dihydroethidium (DHE) and 3–amino,4–aminomethyl–2',7'–difluorescein diacetate (DAF–FM DA), respectively (Beyotime, China). The cells were observed using a fluorescence microscope and the relative fluorescence intensity was analyzed using Image J software. Meanwhile, the cell lysate and culture medium were also collected to quantitatively determine NO production using a Nitric Oxide Assay Kit (Beyotime, China).

S1.7. PSP inhibits the matrix degradation

S1.7.1. The anti–fouling properties of PSP copolymer modified cartilage slices

Synthesis of BSA–FITC: The FITC solution in DMSO (1 mg/mL) was added to a BSA aqueous solution (10 mg/mL). The reaction was maintained in the dark (0 °C, 12 h). Subsequently, the solution underwent dialysis for 3 days. The BSA–FITC product were obtained by dry–freezing.

Preparation of cartilage *slices*: Femur was bought from the supermarket nearby. After separating the bones from the surrounding tissues, including ligaments and muscles, the cartilage was cut into cylindric slices with a diameter of 3 mm and a height of 1 mm.

Anti–fouling determination: The cartilage slices were immersed in a polymer solution (PSB–macroCAT and PSB–*b*–PCOLBP, 1 mg/mL) at 37 °C for 12 h. Subsequently, the modified slices were incubated in a BSA–FITC aqueous solution (100 μg/mL) at 37 °C for 12 h in the dark. After incubation, the slices were removed and the fluorescence intensity of residual solution was detected using a fluorescence spectrophotometer. The anti–fouling ability of zwitterionic polymer–modified cartilage slices was calculated according to formula (8):

$$Anti\text{–}fouling\ ability\ (\%) = \frac{(FL_o - FL_p)}{FL_o} \times 100 \quad (8)$$

where FL_o is the fluorescence intensity of the original protein solution, and FL_p is the fluorescence intensity of post–incubated solution with zwitterionic polymer–modified cartilage slices.

S1.7.2. PSP prevents matrix degradation of chondrocytes

Chondrocytes were seeded in 24–well plates at a density of 30,000 cells/well. After 24 h, the chondrocytes were incubated with PSB and PSP (1 mg/mL) for another 24 h. Subsequently, hyaluronidase (Hyase) or collagenase II (Cls II) (0.5 wt%) were co–cultured with the zwitterionic polymers–treated chondrocytes for 12 h. The live and dead chondrocytes were stained with fluorescein diacetate (FDA) and propidium iodide (PI) dyes, respectively. The nuclei of chondrocytes were stained using Hoechst 33342 solution (10 μg/mL). The staining process was performed with a mixed solution of the three dyes for 10 min. The cell status was then examined using a fluorescence microscope. Chondrocytes treated with Cls II were harvested and stained using the Annexin V–FITC Apoptosis Detection Kit. The live, apoptotic and dead chondrocytes were analyzed quantitatively using a flow cytometer (Millipore Guava EasyCyte 5, France).

S1.7.3. Defence against RAW 264.7 cells

A co–culture system was designed according to a previous study.[2] Chondrocytes were seeded in a 24–well plate at a density of 20,000 cell/well, while RAW 264.7 cells were seeded in cell insert at a density of 5,000 cells/well. After the chondrocytes were incubated with zwitterionic polymers for 24 h, they were cocultured with RAW 264.7 cells. Following another 24 h of cultivation, the cell viability of chondrocytes was measured through CCK–8 assay and live/dead staining.

S1.8. Cell studies

Chondrocytes were cultured in DMEM/F12 medium supplemented with 10% of fetal bovine serum (FBS) and 1% of penicillin–streptomycin (P/S) solution. Bone marrow stromal cells (BMSCs), synovial mesenchymal stem cells (SMSCs), and RAW264.7 cells were cultured in DMEM medium with 10% FBS and 1%. For chondrogenic induction, the medium was supplemented with dexamethasone (0.1 μM), *L*–ascorbic acid (50 μg/mL), *L*–proline (40 μg/mL), sodium pyruvate (100 μg/mL), TGF–β3 (10 ng/mL) and insulin–transferrin–selenic acid (IFS, 1%).

S1.8.1. Isolation of chondrocytes/BMSCs

Chondrocytes were isolated from male Sprague-Dawley (SD) rats (one week old). The rats were euthanized via intraperitoneal injection of an over–dose of chloral hydrate (10%). After sterilization with povidone iodine for 5 min, the knee joints were exposed, and the hyaline cartilage was harvested and cut into piece (approximately 1 mm^3). The cartilage fragments were sequentially incubated in Cls II (0.2%, 0.5 h), trypsin (0.25%, 0.5 h) and Cls II (0.2%, 2 h) at 37 ^oC. The final supernatant was centrifuged at 3000 r/min for 5 min and the obtained chondrocytes were suspended in complete DMEM/F12 medium. Cell passaging was performed when the culture dish was covered with chondrocytes. For the isolation of BMSCs, femurs were collected similarly to the procedure for chondrocytes. The bone marrow aspirate from femur was extracted and filtered through a Corning 70-μm cell stainer, then incubated in a culture dish (d=10 cm). After 3 days of culture, nonadherent cells (primarily blood red cells) were removed. The culture medium was refreshed every 2 days until the cells reached approximately 80% confluence.

S1.8.2. Cytocompatibility

CCK–8 assay: Chondrocytes, BMSCs and SMSCs were seeded in 96–well plate at desities of 5,000 cells/well, 3,000 cells/well and 5,000 cells/well, respectively. After 24 h to allow for cell attachment, the zwitterionic polymers (PSB or PSP) were added to the culture medium. At 24 and 72 h, the culture medium was freshened with CCK–8–supplemented medium (10 vol%) for 3 h of

incubation. The optical density (OD) value of each well was recorded using a microplate reader (KH 360, China). The cell viability was calculated by the following formula (9):

$$Cell\ viability\ (\%) = \frac{OD_e - OD_{eb}}{OD_c - OD_{cb}} \times 100 \quad (9)$$

where OD_e is the OD value of cells incubated with PSB or PSP (experimental group), ODc is the OD value of the free cells (control group), OD_{eb} and OD_{cb} are the OD values of experimental group and control groups' blanks, respectively.

Live/dead staining: The procedure of culture was similar to that of CCK–8 assay. At 24 and 72 h, the cells were stained with a mixture solution of FDA (50 μg/mL) and PI (10 μg/mL) for 15 min. Then, live/dead cells were observed using a fluorescence microscope (Olympus X17, Japan).

Cell morphology staining: At the predetermined time (24 and 72 h), the cells were fixed with 4% paraformaldehyde for 15 min and then treated with Triton X–100 (0.5 vol%) for 5 min to increase the permeability of cell membrane. After washing with PBS for three times, the cells were stained with FITC–labeled phalloidin for 30 min and DAPI solution for 10 min, respectively. The F–actin and nuclei were observed using a fluorescence microscope.

Flow cytometry: Chondrocytes were incubated with PSB or PSP for 24 h. After incubation, the cells were digested and collected through centrifugation (2,000 r/min, 4 min). The cells were then suspended in binding buffer and labeled with Annexin V–FITC/PI according to the instructions of the Annexin V–FITC Apoptosis Detection Kit (Beyotime, China). The live, apoptotic and dead cells were quantitatively analyzed using a flow cytometer.

Apoptotic staining: In brief, chondrocytes, post coculture with polymer–containing medium, were fixed and then stained with Hoechst 33358 (Beyotime, China) for 20 min. The stained cells were observed using a fluorescence microscope.

S1.8.3. Col II–targeting

Apart from chondrocytes and SMSCs that were noted for secreting Col II and Col I, respectively, BMSCs were cultured in a chondro–inducive medium for two weeks. a cell suspension (0.5 mL) containing 100 million cells was mixed with FITC–PSP solution (2 mg/mL, 0.5 mL) for 30 min. Subsequently, the cells and the targeted FITC–PSP were removed by centrifugation (3,000 r/min, 10 min). The supernatant was then diluted with PBS and the fluorescence intensity was measured using a fluorescence spectrophotometer with the extraction/emission wavelength at 490/520 nm, respectively. A similar procedure was carried out using FITC–PSBG for comparison. The targeting efficiency (TE) was calculated through the formula (10):

$$TE\ (\%) = \frac{(FL_{fzp} - FL_s)}{FL_{fzp}} \times 100 \quad (10)$$

where the FL_{fzp} is the fluorescence intensity of FITC–labeled zwitterionic polymers, and FL_s implies the fluorescence intensity of the supernatant of the culture medium after centrifugation.

S1.8.4. Cell autophagy

Chondrocytes, BMSCs and SMSCs were seeded in 24–well plates and co–cultured with zwitterionic polymers (1 mg/mL) for 24 h. To induce autophagy, cells treated with 3 Earle's Balanced Salt Solution (EBSS) solution for 2 h were designed as the "Autophagy+" group. Subsequently, cells were stained using Autophagy Staining Assay Kit, which includes monodansylcadaverine (MDC) and PI. The stained cells were observed using a fluorescence microscope to evaluate autophagic activity.

S1.8.5. Chondroprotection

RNA sequencing: After LPS induction for 1 d, chondrocytes were cultured with PSB or PSP–supplemented medium for 1 week. Subsequently, chondrocytes were digested, and total RNA was extracted using Trizol agent (ThermoFishier, USA) following the manufacturer's instructions The RNA collection, detection and data analysis were conducted by Novogene Biotech Co., Ltd (Beijing, China) through illumine Nova–seq 6000 platform (illumine, USA) platform. Differentially expressed genes (DEGx) were identified based on the criteria: padj < 0.05 and |fold change| > 2.

Real–time quantitative polymerase chain reaction (RT–qPCR): The total RNA was extracted using Trizol agent (ThermoFisher, USA), followed by determination of RNA concentration. Reverse transcription was performed using the PrimerScirpt^{TM}RT Reagent Kit. Subsequent PCR reactions were carried out, with the specific details provided in Table S3. Relative gene expressions were quantified using the $2^{-\Delta\Delta CT}$, where CT indicated cycle threshold.

ELISA assays: Follwing similar procedures as used in the RNA sequencing assay, cell was lysed using a 0.1 vol% Triton X–100 solution. After centrifugation at 10,000 r/min for 10 min at 4 ^{o}C, the supernatant was collected and stored at –20 ^{o}C until further analysis. The concentration of intracellular IL–6, TNF–α, PGE–2, Col II and Aggrecan were analyzed using the respective ELISA kits (Bioswamp, Wuhan, China).

Immunohistochemical (IHC) staining: The expression of aggrecan and Col II in chondrocytes was investigated using IHC staining. Briefly, chondrocytes were treated with the anti–aggrecan

antibody and anti–Col II antibody during IHC staining. The relative expression levels of aggrecan and Col II expression in cytoplasm were quantified using Image J software, based on at least three randomly selected images.

Safranin–O/fast green (SF) staining: The expression of cartilage matrix in chondrocytes was characterized using Modified Safranine O–Fast Green Cartilage Stain Kit. Briefly, chondrocytes on cell climbing tablets were fixed with 4% paraformaldehyde for 20 min. The fixed cells were then stained with the Weigert solution (5 min) and subsequently washed with H_2O. Following this, the cells were stained with fast green solution (5 min) and safranin–O solution (5 min), respectively. After staining, the cells were washed briefly with a weak acid solution for 15 s and dehydrated before observation.

Histological staining: After LPS induction and incubation with polymers (PSB and PSP), the chondrocytes were fixed with 4% paraformaldehyde and then stained using periodic acid–schiff (PAS) staining solution. The stained cells were then imaged using an optical microscope. Similarly, Alcian blue staining was performed to characterize the biosynthesis of HA.

S1.9. Animal studies

Male SD rats (6 weeks old) were source from the Experimental and Research Animal Institute (Sichuan University, China). All animal studies were conducted with the approval of the Medical Ethics Committee (No. KS2020028), and were performed at Experimental and Research Animal Institute of Sichuan University. The rats were provided with unrestricted access to food and maintained under a 12–h dark/light cycle.

S1.9.1. *In vivo* degradation–resistance analysis

Prior to intraarticular (I.A.) injection of catabolic enzymes (Hyase or Cls II), the polymers (PSB and PSP) were injected into the joint cavity. After treatment with catabolic enzymes, femurs were collected for detailed histological staining and Immunohistochemical staining.

S1.9.2. In vivo OA therapy

Surgical OA model: The OA model was established following a previously reported protocol.[3] Briefly, 15 male rats (12 weeks old) were anesthetized with isoflurane. Subsequently, the right joint was subjected to transection of the medical meniscotibial ligament. After ensuring proper suturing of the wound, the rats were allowed free access to water and food.

Administration of zwitterionic diblock polymer: A week after surgery, all the rats (5 healthy rats and 15 OA rats) were divided into 4 groups (n = 5 per group). When rats were anesthetized with isoflurane, each group received I.A. injections of by 50 μL of either saline (Normal and OA groups), PSB (1 mg/mL) or PSP (1 mg/mL) once every two weeks. The treatment was continued for 8 weeks. Following the treatment period, blood and femurs were harvested to evaluate both biosafety and therapeutic effect.

S1.9.3. Microcomputed tomography (micro–CT) assessment

Micro CT was utilized to evaluate the repaired femurs. Femur specimens were scanned using a micro–CT system (VGS tudio Max software) with a scanning current of 130 μA and a voltage of 70 kV. Detailed analysis of femurs was performed by reconstructing three–dimensional (3D) structures and calculating the osteophyte volumes. This approach enabled precise quantification of bone morphology and the extent of osteophyte formation, providing valuable insights into the efficacy of the treatments.

S1.9.4. Histological and immunohistochemical analysis

The femurs and major organs (heart, liver, spleen, lung and kidney) of the rats were harvested to evaluate both the therapeutic effect on OA and systematic biosafety. All samples were fixed in a 10% formalin solution. The femurs specimens were subjected to decalcification before further measurements. Subsequently, the samples were embedded in paraffin and sectioned into thin slices for histological examination.

H&E staining: The sections (femurs and major organs) were stained with hematoxylin and washed with H_2O and EtOH (95%), respectively. Subsequently, they were stained with erosin Y solution (1%, 3 min).

Masson staining: The sections were stained using the Masson's Trichrome Stain Kit under the manufacturer's instructions.

Safranin–O/fast green staining: The sections of femurs were stained with Weigert's hematoxylin solution (10 min), and then stained with fast green solution (5 min). After being rinsed by acetic acid (1%), the sections were further stained with Safranin–O solution (0.1%, 5 min).

IHC staining: The IHC staining of Col II were performed with similar measurements to that in cell study described above.

S1.9.5. Histopathology assessment of OA therapy of PSP

The histologic grading of cartilage destruction was evaluate using both the Osteoarthritis Research Society International (OARSI) scoring system and Mankin's method (including structures, cells, matrix and total evaluation). Additionally, the macroscopic appearance of cartilage was assessed using the International Cartilage Repair Society (ICRS) scoring system to determine the integrity of repaired cartilage.

$$Therapeutic\ effect(\%) = \frac{S_{OA} - S_E}{S_{OA}} \times 100 \quad (11)$$

Where S_{OA} and S_E were the OARSI scores of the OA and experimental groups, respectively.

S1.10. Statistical analysis

All data were shown as mean ± standard deviation (SD), and all experiments were repeated at least 3 times. Shapiro–Wilk test was utilized to analyze the normality of the data distribution As for data without a Gaussian distribution and categorical data (including OARSI, Mankin's score and ICRS score), non–parametric method (Kruskal–Wallis test) was performed. To assess the homogeneity of cariances for data with a Gaussian distribution, the F–test was employed. For multiple comparisons of data with both Gaussian distribution and euqal variances, ordinary one–way analysis of variance (ANOVA) was performed. For groups with unequal variances, the Brown–Forsythe and Welch ANOVA tests were performed. Post–hoc tests with Bonferroni correction were conducted for pairwise comparisons following ANOVA. An unpaired two–tailed t–test was performed to analyze the significance of difference between two groups. Statistical significance was considered at $p < 0.05$. All Statistical analysis was performed using Graphpad Prism 8.02.

S2. Supplementary results and discussion

S2.1. Synthesis and characterization of methacrylic acid N–hydroxysuccinimide ester (NHSMA)

The chemical shift at 2.85 ppm corresponds to the methene of the NHS ester, while peaks at 6.39 ppm and 5.86 ppm indicate the presence of double bonds. The peak at 2.04 ppm is indicative of a methyl group (Figure 1b). In the ^{13}C NMR spectra, the chemical shifts observed at 19, 131, 132 and 170 ppm further confirm the successful synthesis of NHSMA (Figure S1a). The FT–IR spectra (Figure S1b–c) reveal bands at 944 cm^{-1} and 981 cm^{-1}, referring to out–of–plane deformation vibration of C–H in R–CH=CH(CH_3). The bands at 1632 cm^{-1} indicates C=C stretching vibration, and the bands at 3003 cm^{-1} signifies C–H stretching vibration of the vinyl ester. These spectral features collectively affirm the successful chemical modification of NHS with methacrylic acid ester.

S2.2 Synthesis and characterization of lubricin–inspired deblock poly (sulfobetaines)–*co*–poly (collagen II–binding peptide) (PSBMA–*co*–PColBP, PSP)

The ColBP is grafted onto PSN in weak basic conditions, resulting in the formation of the final PSP copolymer. The reducibility of Trp/Tyr residues in ColBP adds an advantageous dimension, promising the manifestation of lubricating, anti–oxidative, and anti–degradation properties. Consequently, the rational design of PSP with chondroprotection properties in the inflammatory environments aligns with contemporary strategies for enhancing therapeutic interventions in the context of osteoarthritis.

To mimic the binding domain of natural lubricin, ColPB is grafted onto PSN through the highly reactive amide formation between amino groups of hexapeptide and the reactive esters groups of PSN. The successful replacement of NHS groups by ColBP is evidenced by the disappearance of NHS's characteristic peaks and the emergence of amide I peaks (Figure S2). Quantitative analysis reveals an increment in N1s (from 5.92% in PSN to 6.61% in PSP) and a decrease in S2p (from 5.21% in PSN to 5.09% in PSP) (Table S1), affirming the success in peptide conjugation. This is further substantiated by the elevated N–C=O/C–N contents (Figure S3 and S6). Unlike PSB and PSN, PSP displays a UV absorbance at 280 nm, attributed to the W and Y residues in ColBP (Figure S7). Moreover, ColBP exhibits FL intensity at 340 nm (Figure S8), whereas NHS aggregates display FL intensity at 570 nm. The observed increase in FL intensity at 340 nm and the concurrent reduction at 570 nm (Figure S9) confirms the successful peptide conjugation. The bioactivity of hexapeptide is intricately linked to its conformation. As shown in Figure S10, PSB and PSN has no CD signals, while PSP demonstrates signals comparable to those of ColBP, suggesting that the amide reaction under weak basic conditions has minimal influence on the peptide conformation. Precise quantification using a BCA assay kit reveals the Col BP content in PSP to be 0.04 g/g (Figure S11). In all, these comprehensive data collectively affirm the successful synthesis of lubricin–inspired PSP as designed.

S2.3. Col II–targeting property of WYRGRL

The FITC–labeled ColBP exhibits a stronger affinity for Col II compared to HA and CS, as evidenced by of higher fluorescence intensity (Figure S12). Molecular docking studies further corroborate this finding, revealing binding affinities of –6.11 kcal/mol, –3.79 kcal/mol and –3.97 kcal/mol for WYRGRL to Col II, CS and HA, respectively (Figure S13). These results highlight the special targeting property of WYRGRL toward Col II within the cartilage matrix.[4] This affinity

is crucial for enhancing the therapeutic potential in cartilage repair and regeneration, providing a more targeted approach in the treatment of cartilage-related disorders.

S2.4. PSP protects cartilage matrix against degradation enzymes

Benefiting from the chondroprotection conferred by targeted PSP, both Hyase and Cls II are rendered ineffective in degrading the cartilage matrix (Figure S18 and S20). This protection ensures that the cartilage is shielded from abnormal friction forces, maintaining a smooth surface and demonstrating effective resistance to degradation. Immunohistochemical staining of Col II (Figure S19) and histological staining of HA (Figure S21) visually confirm matrix loss in cartilages treated with catabolic enzymes or pretreated with PSB. In contrast, cartilage pretreated with PSP retains its normal matrix composition, highlighting the superior protective effect of PSP against enzymatic degradation.

S2.5. Anti–friction properties of PSP as lubricants

Under a low loading force (1 N) and a sliding frequency of 0.5 Hz, the coefficient of friction (COF) is observed to be the lowest, approximately 0.034 (Figure S22). For PSB, the polymer chains tend to tangle, promoting the formation of intramolecular and intermolecular ionic and hydrogen bonds. However, there are no additional interactions to enhance the interface binding to the PTFE plate and Al_3O_2 ball. Consequently, the hydration ability of the polymers is reduced, leading to an increased COF as the sliding frequency increases. In contrast, the introduction of ColBP in PSP induces hydrophobic interactions and metal–phenol interactions, contributing to a stable hydration layer. This results in minimal COF fluctuations with changes in sliding frequency in the PSP group, suggesting that PSP exhibits characteristics consistent with boundary lubrication. These data affirm that PSP is a promising candidate for restoring the lubrication capacity of damaged cartilage induced by OA.

S2.6. Targeted lubrication properties of PSP on the cartilage surfaces in knee joints

In knee joint cartilages, the COF is observed to be the highest across all sliding frequencies (Figure S24). Preincubation with PSBG, which adheres to the surface through multiple weak interactions, results in a slight decrease in the COF. However, cartilages treated with PSP show the lowest COF, ranging from 0.016 to 0.021. This significant reduction in COF suggests that PSP is highly effective in enhancing the lubrication properties of knee joint cartilage, potentially offering improved joint function and protection against OA–induced damage.

S2.7. Biocompatibility of PSP

The CCK–8 assays demonstrate good cell viability (>83.60%) and normal proliferation of chondrocytes/BMSCs/SMSCs when co–cultured with PSB and PSP (Figure S37a, S38a and S39a). Live/dead staining images (Figure S37b, S38b and S39b) reveal numerous green cells with almost negligible red cells, suggesting that incubation with PSB and PSP does not induce cell death. Moreover, the spread morphology of cells (Figure S37c, S38c and S39c) indicates the normal expression of F–actin, which is essential for biological activities and cell movements. The assessment of lactic dehydrogenase (LDH) release, an indicator for biocompatibility,[5] exhibits no significant difference, indicating intact cell membrane for both PSB and PSP (Figure S40). Flow cytometry analysis further details the state of cell growth, revealing that while there are apoptotic and dead cells in PSB and PSP groups, the majority remains in the early apoptosis state, with the apoptotic/dead cell ratio significantly smaller than that of live cells (Figure S41). Collectively, these findings confirm the desirable biocompatibility of PSB and PSP.

As shown in Figure S42a, chondrocytes in the OA joint are typically influenced by inflammatory cells. To evaluate the biocompatibility of PSP in simulative OA microenvironments, a co–culture system based on a transwell setup has been developed. In the presence of RAW264.7 cells, which exert adverse effects, the cell viability of chondrocytes and SMSCs reduces to 72% and 52%, respectively (Figure S42b–c). Although PSB exhibits good biocompatibility, it fails to alleviate the inflammation invasion of RAW 264.6 cells due to its inadequate anti–oxidation/degradation–resistance properties, resulting in relatively low cell viability (73% and 69% for chondrocytes and SMSCs, respectively). Conversely, PSP is anticipated to repel inflammatory cytokines secreted by RAW 264.7 cells and scavenge overproduced ROS/RNS. This results in a beneficial impact on chondrocytes and SMSCs in the co–culture system, with significantly higher cell viability (>84%) compared to PSB group, as well as a greater number of live cells (Figure S42d). In short, the synergistical effect of ColBP and sulfobetaine polymers has enhanced the biocompatibility of PSP in the inflammatory microenvironment.

S2.8. The gene expressions of PSP–treated chondrocytes

The detailed analysis of relative mRNA expression for adatms5, MMP–13, acan and Col2a1, is conducted using RT–qPCR. The results reveal a significant upexpression of adamts–5 in both LPS and PSB groups compared to control ($p < 0.01$) and PSP ($p < 0.01$) groups (Figure S45a), indicating the PSB is ineffective in addressing the overexpression of adamts–5. In contrast, PSP

exhibits potential in inhibiting proteoglycan loss, suggesting a therapeutic prospect for OA reversal. Regarding MMP–13 expression, both PSB and PSP groups exhibit statistically lower levels compared to the LPS group ($p < 0.001$, Figure S45b). This implies that both PSB and PSP can counteract the effects of LPS, with zwitterionic moieties playing a vital role in suppressing MMP–13 expression. In the context of chondrogenesis, the LPS–activated inflammatory response interferes with the expression of acan and Col2a1 (Figure S45c–d). PSP demonstrated an upregulation of acan expression, comparable to that in the control group, and a significantly higher expression of Col2a1 compared to the LPS group ($p < 0.01$). Conversely, PSB does not show the same effectiveness. These findings confirm that PSP contributes to chondro–protection by down–regulating catabolic components (adamts–5 and MMP–13) and up–regulating anabolic components (acan and Col2a1).

S2.9. PSP alleviates inflammation response

Interleukin–6 (IL–6) is a well–known proinflammatory cytokine involved in degradation of cartilage matrix, compromising the structural integrity of cartilage by up–regulating the expression of matrix metalloproteinases (MMPs).[6] Accordingly, various inflammatory factors such as prostaglandin E2 (PGE–2) and tumor necrosis factor–alpha (TNF–α) are significantly elevated in inflammatory conditions. PEG–2 promotes the accumulation of intercellular cAMP, leading to increased osteoclast formation and accelerated chondrocytes apoptosis, which contributes to joint pain.[7] TNF–α triggers a cascade amplification reaction, promoting cartilage degradation, disrupting joint homeostasis and exacerbating OA.[8] As shown in Figure S46, LPS has increased the expression of IL–6, PGE–2 and TNF–α in chondrocytes. However, incubation with PSP mitigates the inflammatory response. PSP, with its capacity to scavenge ROS/RNS and repel catabolic enzymes, effectively inhibits the inflammation response. This is evidenced by the expression levels of inflammatory cytokines in the PSP group being comparable to those in the control group. Consequently, PSP acts as a protective shield to alleviate the catabolic pathological process associated with inflammatory response.

S3. Supplementary Figures

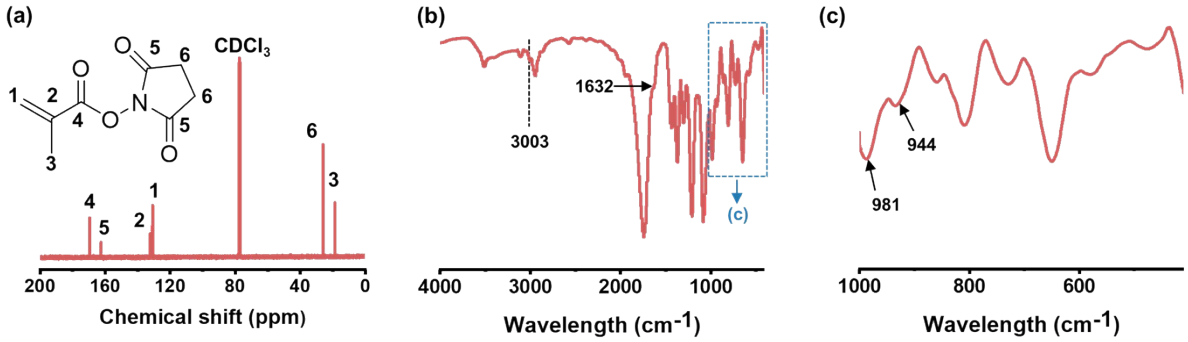

Figure S1 (a) 13C NMR spectra, and (b–c) FT–IR spectra.

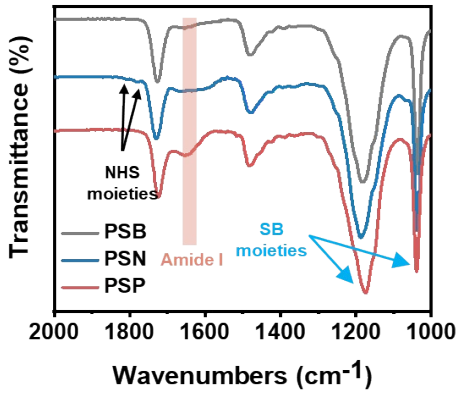

Figure S2 The FT–IR spectra of PSB, PSN and PSP.

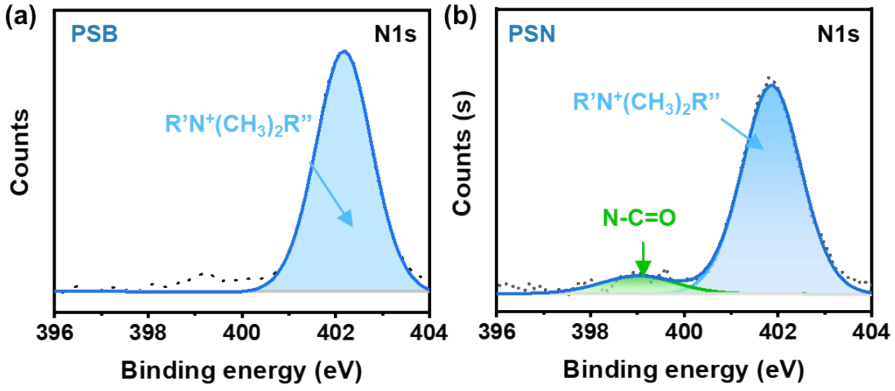

Figure S3 The N1s core–level spectra of (a) PSB and (b) PSN.

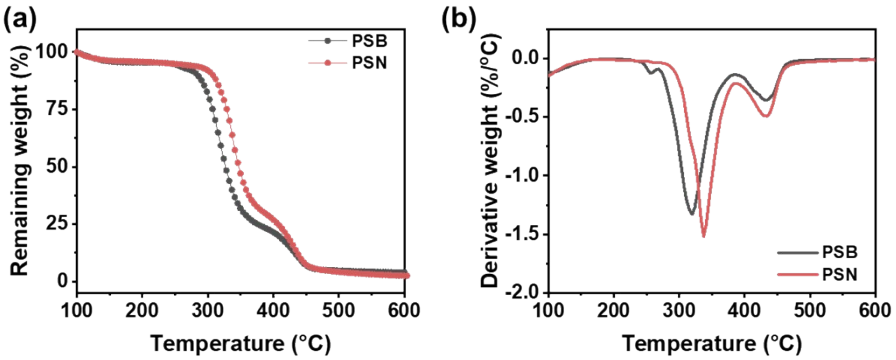

Figure S4 (a) The thermogravimetry analysis (TGA) curves, and (b) derivative thermogravimetry (DTG) curves of PSB and PSN.

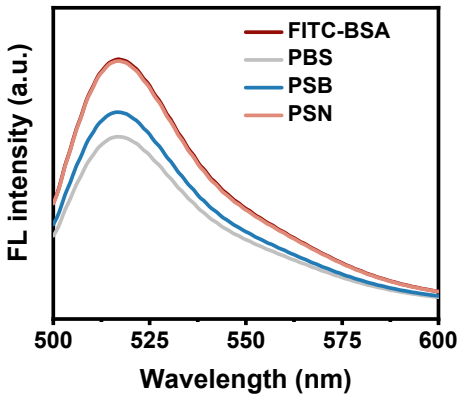

Figure S5 The fluorescence intensity FITC–BSA solution and FITC–BSA solution treated by pristine cartilage slices (PBS), PSB–treated and PSP–treated cartilage slices.

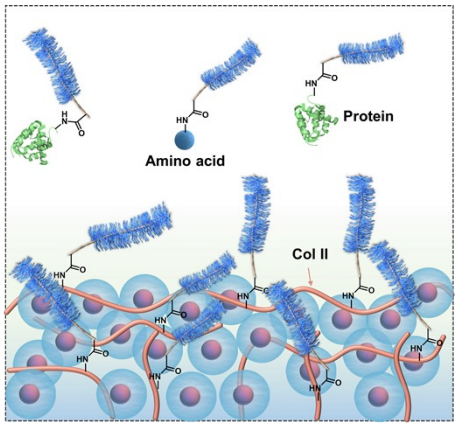

Scheme S1 Rapid conjugation of PSN to various amine–incorporated molecules (amino acid, secreted proteins and Col II) in the microenvironment of chondrocyte growth.

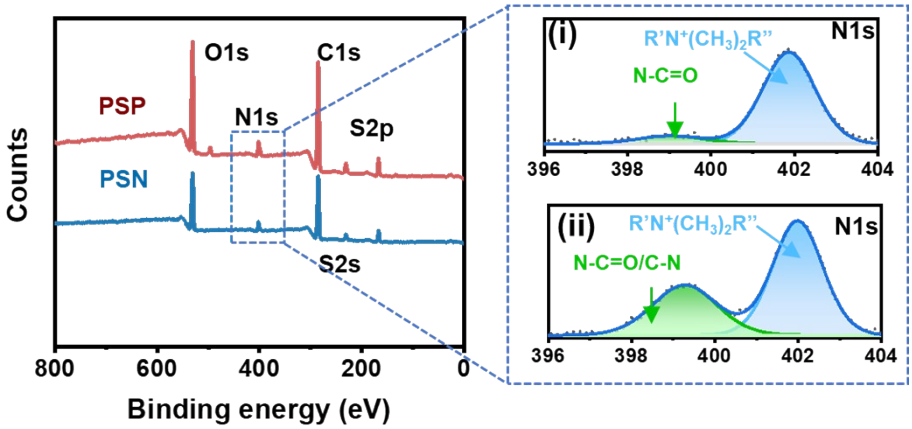

Figure S6 The XPS spectra of PSN and PSP. The N1s core–level spectra of (i) PSP and (ii) PSN.

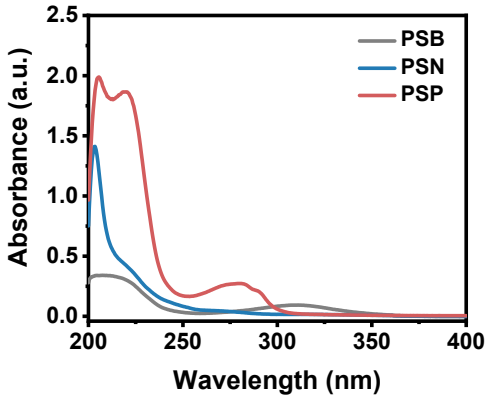

Figure S7 The UV spectra of PSB, PSN and PSP.

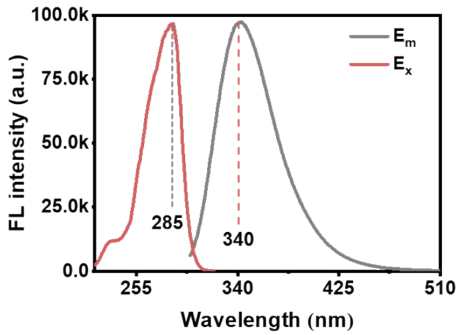

Figure S8 The fluorescence intensity of WYRGRL hexapeptide: excitation wavelength at 285 nm and emission wavelength at 340 nm.

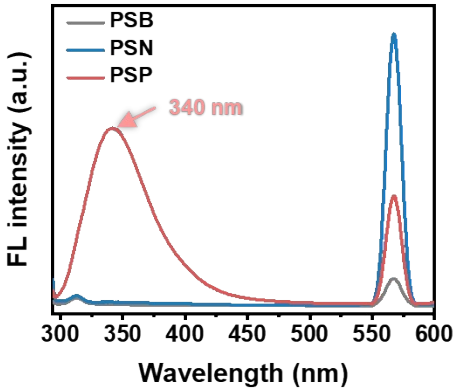

Figure S9 The fluorescence intensity of PSB, PSN and PSP.

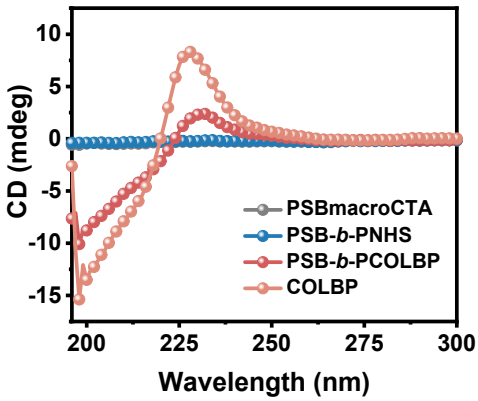

Figure S10 The CD spectra of PSB, PSN, PSP and Col BP.

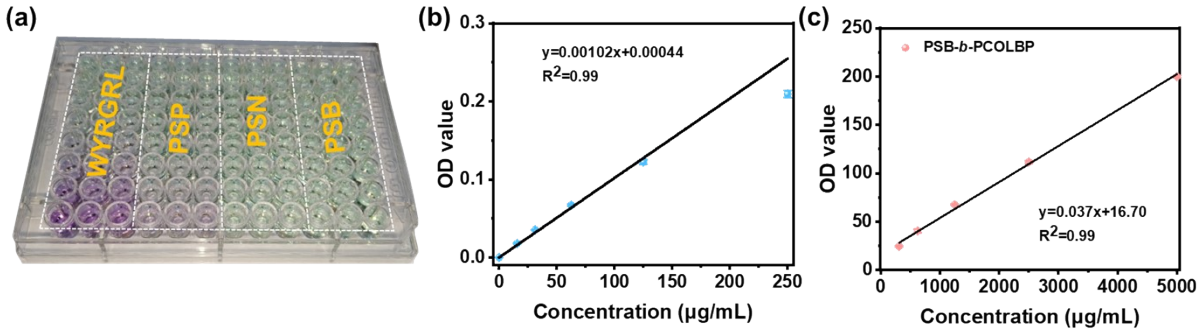

Figure S11 (a) The chromogenic reaction of WYRGRL hexapeptide through BCA Assay Kit. (b) The standard curve of WYRGRL and (c) the quantitative analysis of ColBP content in PSP.

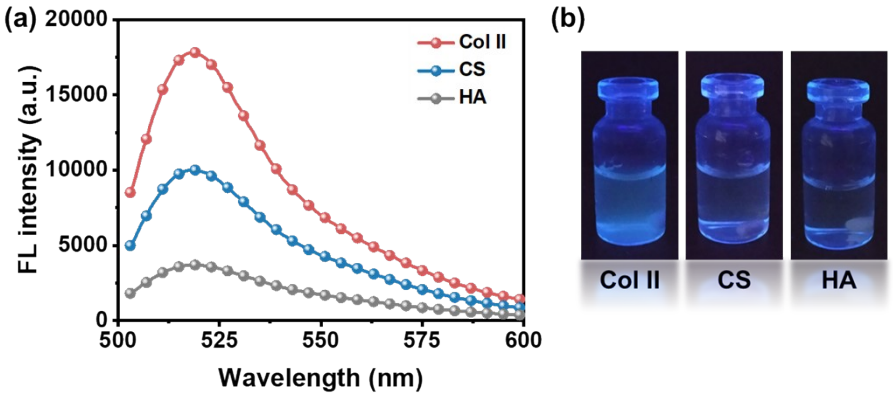

Figure S12 The selective binding of FITC–labelled ColBP to Col II. (a) Fluorescence intensity of Col II, CS and HA solution which were pre–interacted with FITC–labelled ColBP. (b) The corresponding photographs.

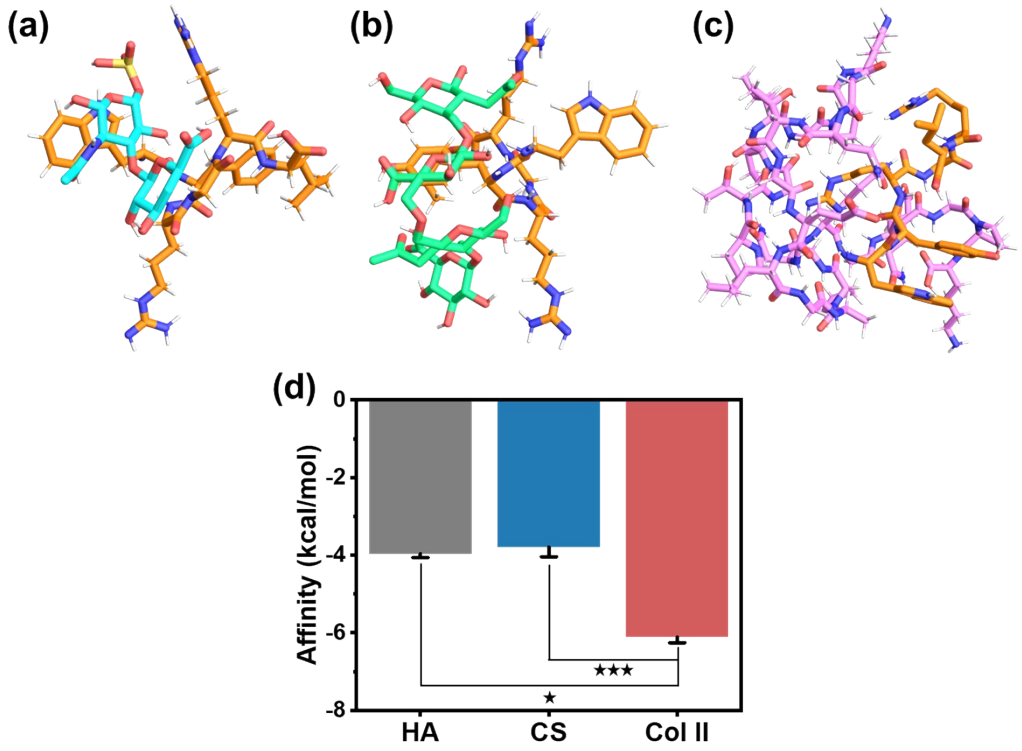

Figure S13 Molecular docking between WYRGRL peptide and biomacromolecules in cartilage matrix: (a) WYRGRL and hyaluronic acid (HA), (b) WYRGRL and chondroitin sulfate (CS), (c) WYRGRL and Col II, and (d) quantitative affinity. * ($p < 0.05$) and *** ($p < 0.001$) suggest significant difference.

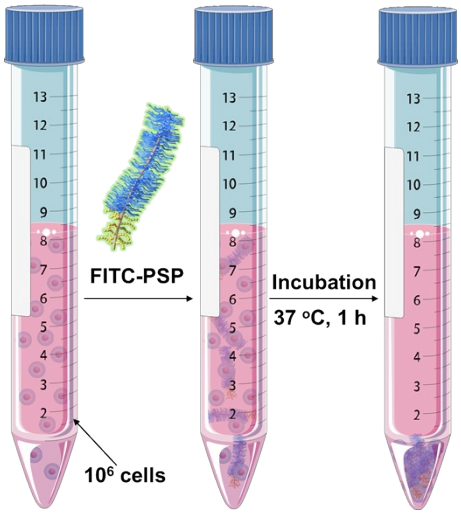

Scheme S2 The illustration of procedures for determining the targeting efficiency to two copolymers (PSBG and PSP).

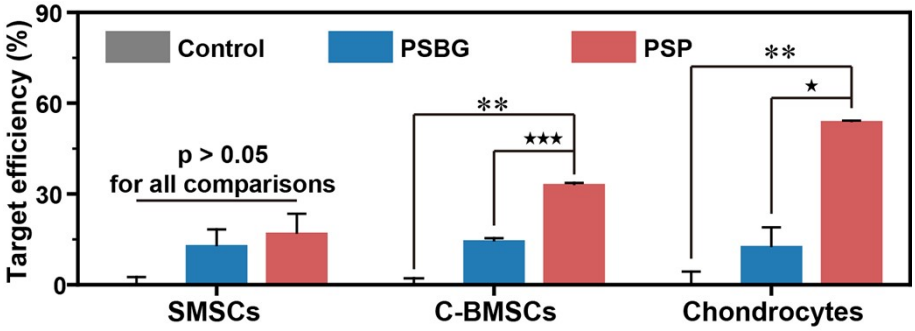

Figure S14 The target efficiency of PSBG and PSP toward different cells (SMSCs, C–BMSCs and chondrocytes). ** ($p < 0.01$) indicates significant difference compared with the control group. ★ ($p < 0.05$) and ★★★ ($p < 0.001$) imply statistical difference between PSBG and PSP groups.

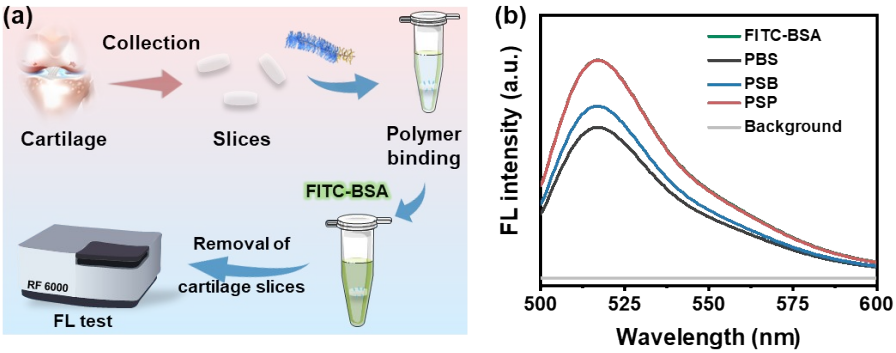

Figure S15 (a) Schemes of experimental process and (b) the fluorescence solutions with various treatments.

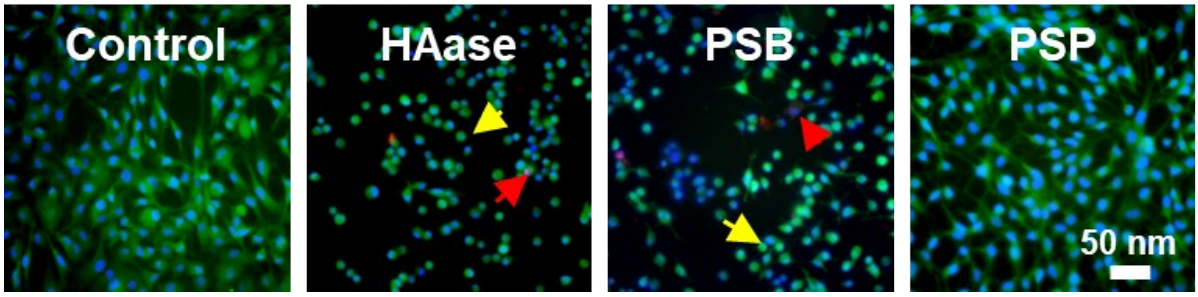

Figure S16 Live/dead/nuclei staining images of control, Hyase, PSB and PSP groups. The red yellow and red arrows suggest live and dead cells, respectively.

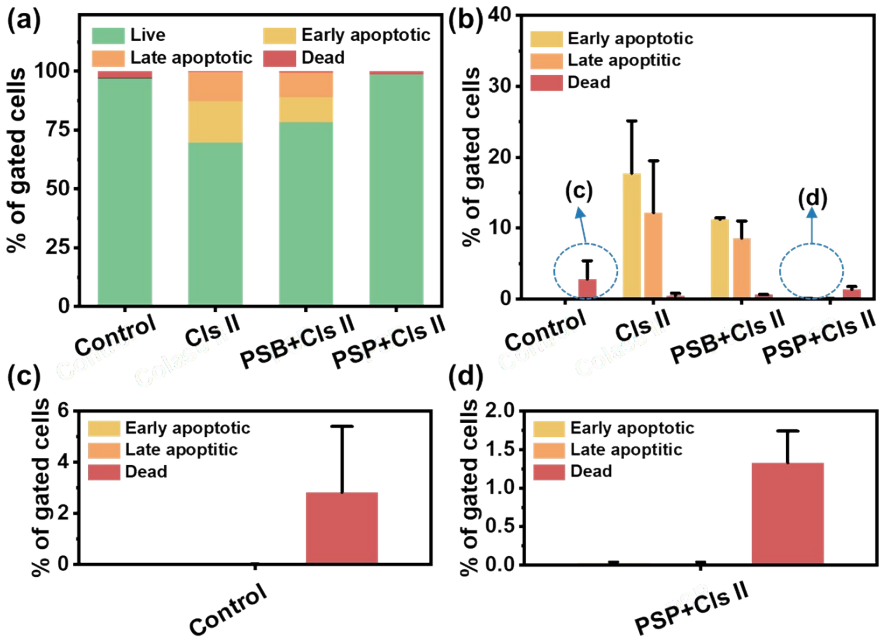

Figure S17 The flow cytometry analysis of chondrocytes incubated with PSB and PSP followed by Cls II invasion. (a) Percentage of live, early apoptotic, late apoptotic and dead cells, and (b) the quantitative illustration of percentage of apoptotic cells. (c) The details of dead of apoptotic cells of control group. (d) The details of dead of apoptotic cells of PSP group.

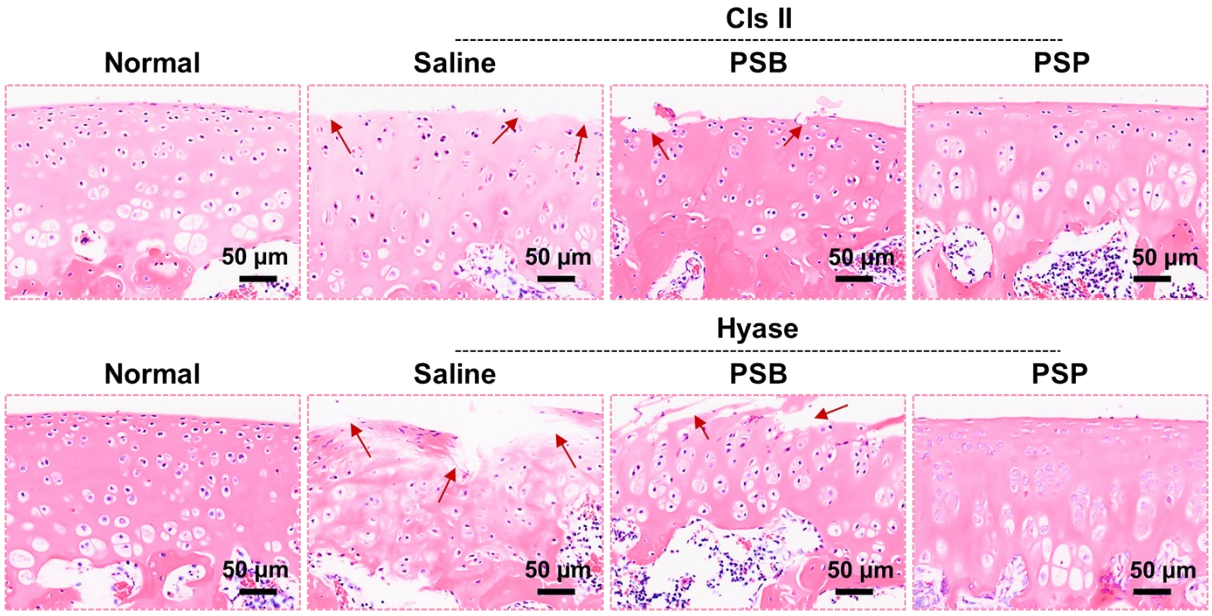

Figure S18 H&E staining slices of femur treated with zwitterionic polymers (PSB and PSP) and catabolic enzymes (Cls II and Hyase), respectively. The red arrows indicate fissures of cartilage.

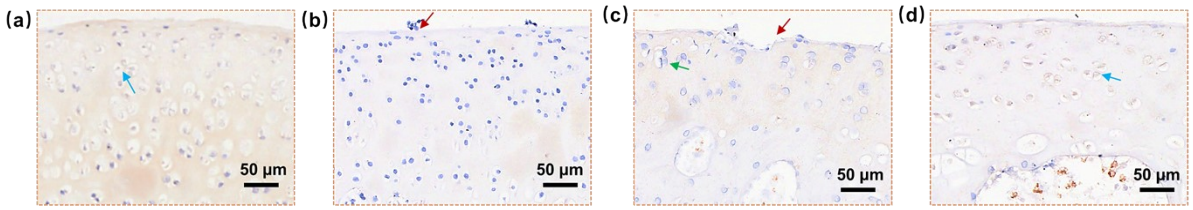

Figure S19 Immunohistochemical staining of Col II: (a) normal, (b) Cls II, (c) PSB+Cls II and (d) PSP+Cls II groups. The blue arrows indicate chondrocytes with positive expression of Col II, the red arrows refer to fissures of cartilage and clusters of chondrocytes, and the green arrow suggests chondrocytes with negative expression of Col II.

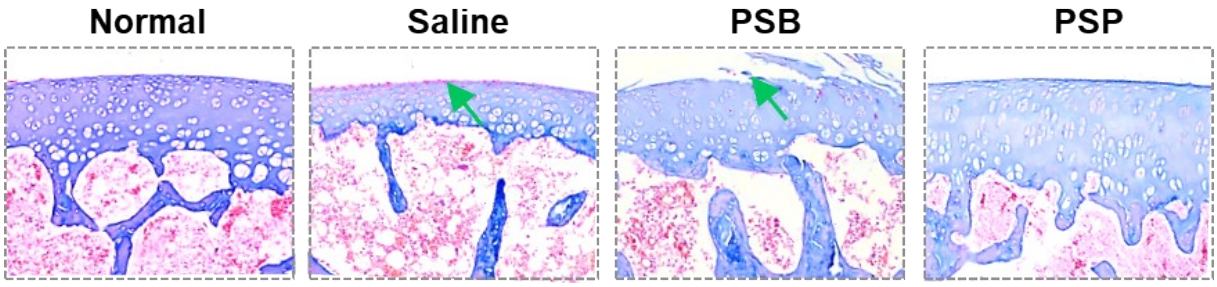

Figure S20 The Masson's staining images of femur treated with zwitterionic polymers (PSB and PSP) and Hyase, respectively. The green arrows indicate fissures of cartilage surface.

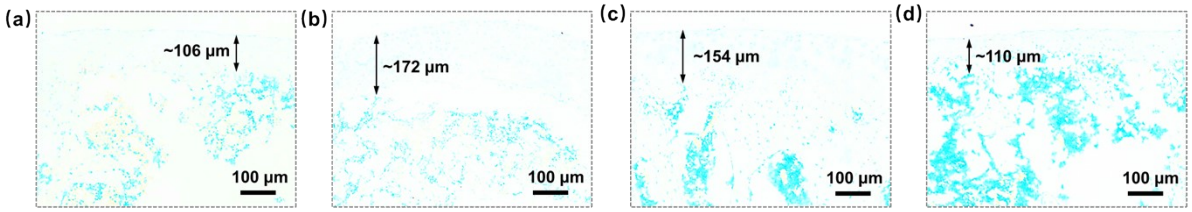

Figure S21 HA staining slices of femur: (a) normal, (b) Hyase, (c) PSB and (d) PSP treated. The distance of absent HA staining of normal, HAsae, PSB and PSP is 106 μm, 172 μm, 154 μm and 110 μm, respectively.

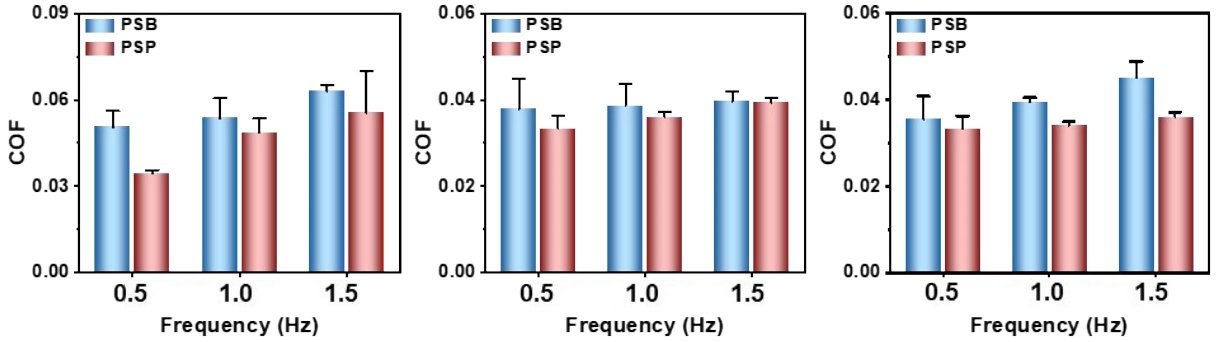

Figure S22 The coefficient of friction (COF) of PSB and PSP as biolubricants with the load forces at 1 N, 2 N and 3 N.

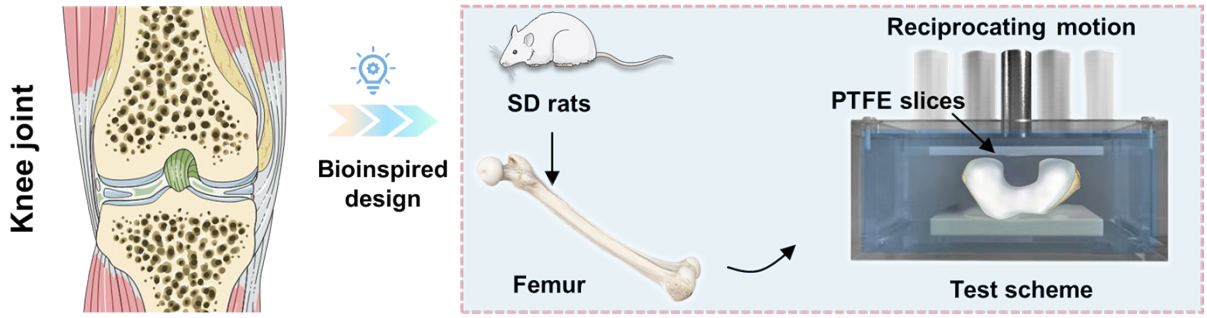

Scheme S3 The *ex vivo* COF tests using femurs.

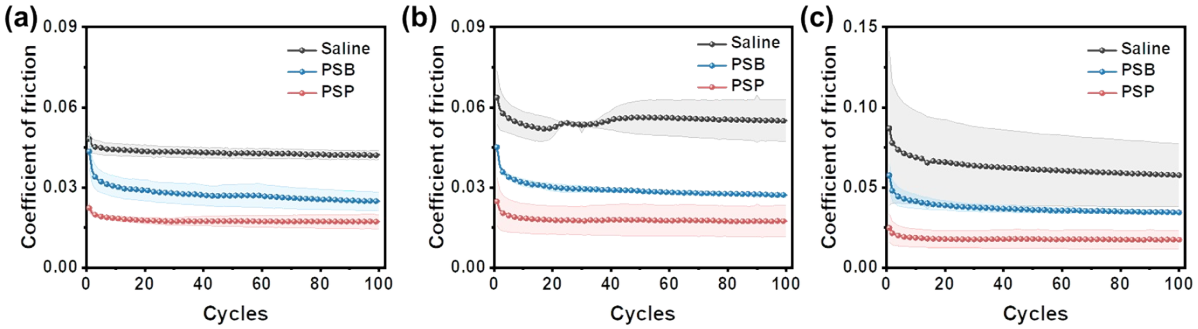

Figure S23 The changes of coefficient of friction of femur pretreated with saline, PSBG and PSP. The sliding frequency is (a) 0.5 Hz, (b) 1.0 Hz and (c) 1.5 Hz.

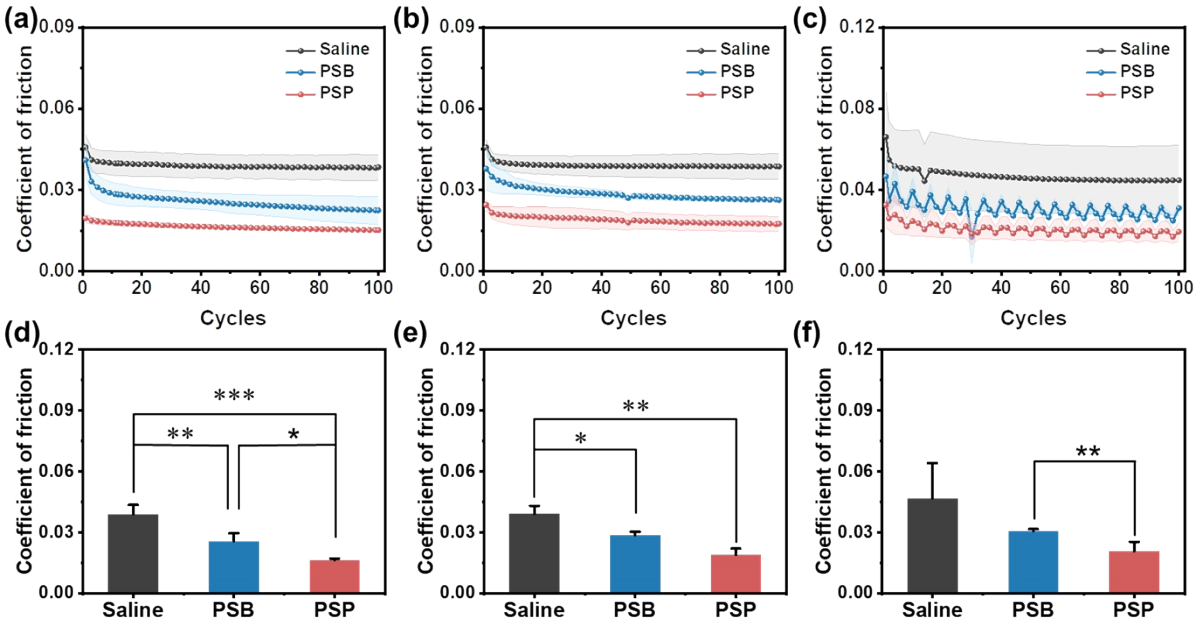

Figure S24 The changes of COF and the average COF of PSP–targeted femur with the sliding frequency as (a, d) 0.5 Hz, (b, e) 1.0 Hz and (c, f)1.5 Hz. * ($p < 0.05$), ** ($p < 0.01$) and *** ($p < 0.001$) indicate the significant difference in comparison to the saline groups. ★ ($p < 0.05$) and ★★ ($p < 0.01$) imply statistical difference between PSBG and PSP.

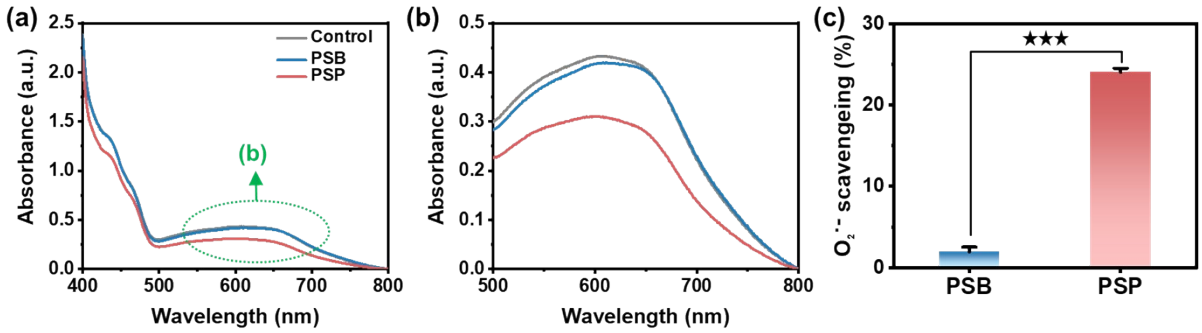

Figure S25 O·– 2 scavenging ability of PSB and PSB. The UV–vis spectra within the range of (a) 400–800 nm and (b) 500–800 nm. (c) The O·– 2 scavenging ratios of PSB and PSP. ★★★ (p < 0.001) refers to the significant difference.

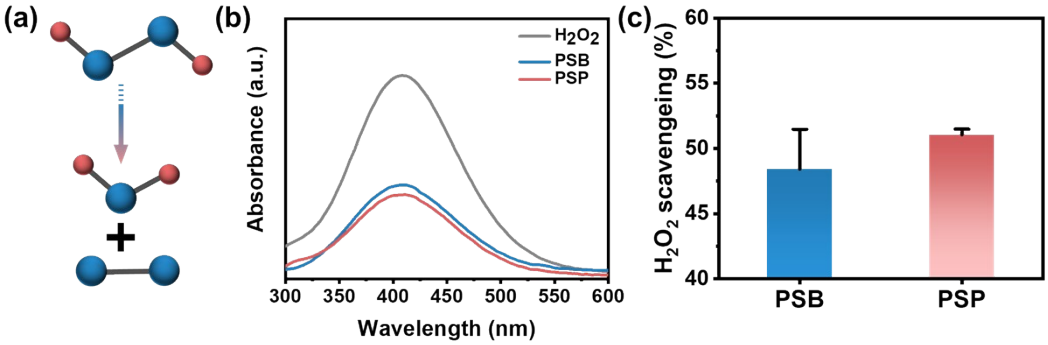

Figure S26 The CAT–like activity of PSB and PSP to scavenge H_2O_2. (a) Scavenging mechanism and (b) UV–vis spectra between 300 to 600 nm. (c) The H_2O_2 scavenging ratio of PSB and PSP.

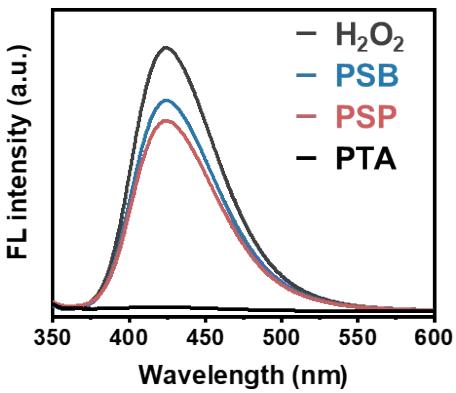

Figure S27 The ·OH scavenging capacity of PSB and PSP.

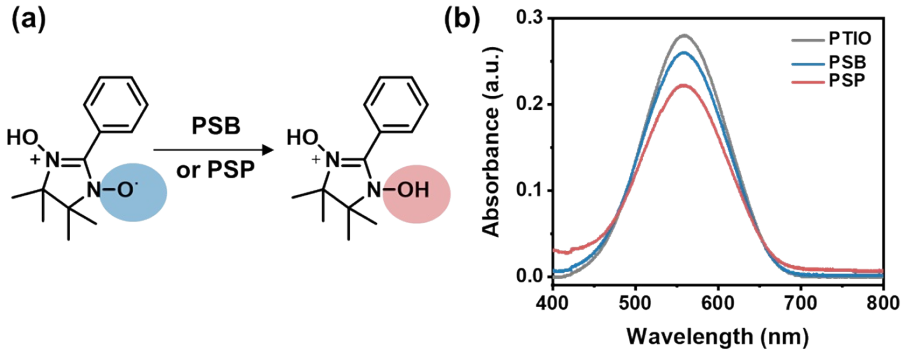

Figure S28 The PTIO scavenging ability of PSB and PSP. (a) The chemical mechanism of scavenging radical and (b) UV–vis spectra between 400 to 800 nm.

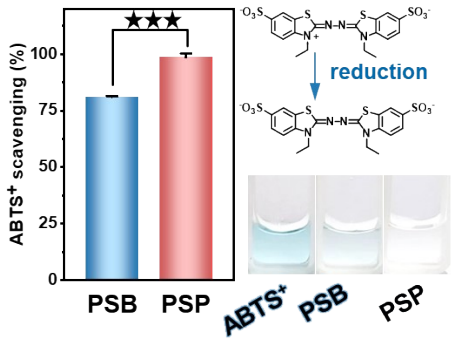

Figure S29 The $ABTS^+$ scavenging property of PSB and PSP. ★★★ ($p < 0.001$) refers to the significant difference.

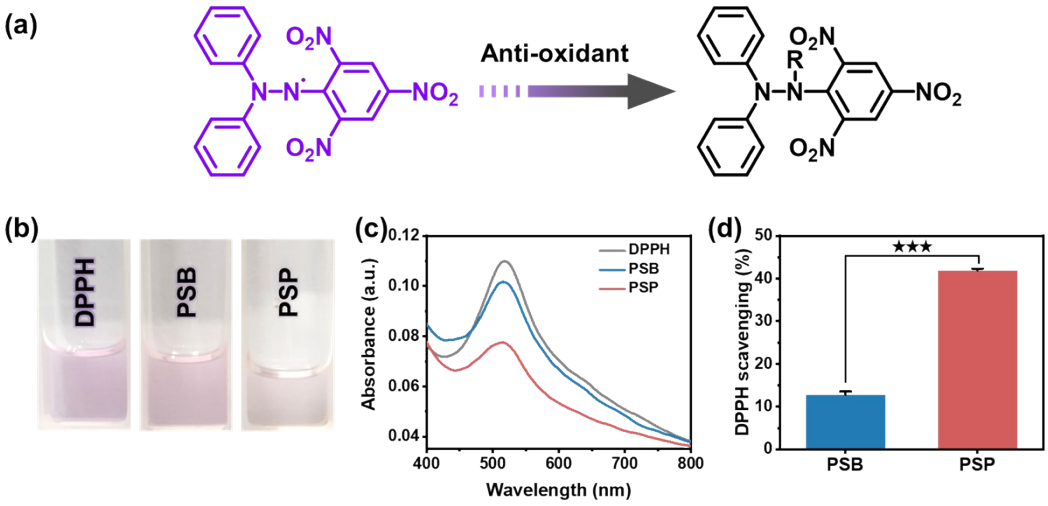

Figure S30 The DPPH scavenging ability of PSB and PSP. (a) Scavenging mechanism, (b) visual photographs, (c) UV–vis spectra between 400 to 800 nm and (d) quantitative DPPH scavenging ratio. ★★★ ($p < 0.001$) indicates significant difference.

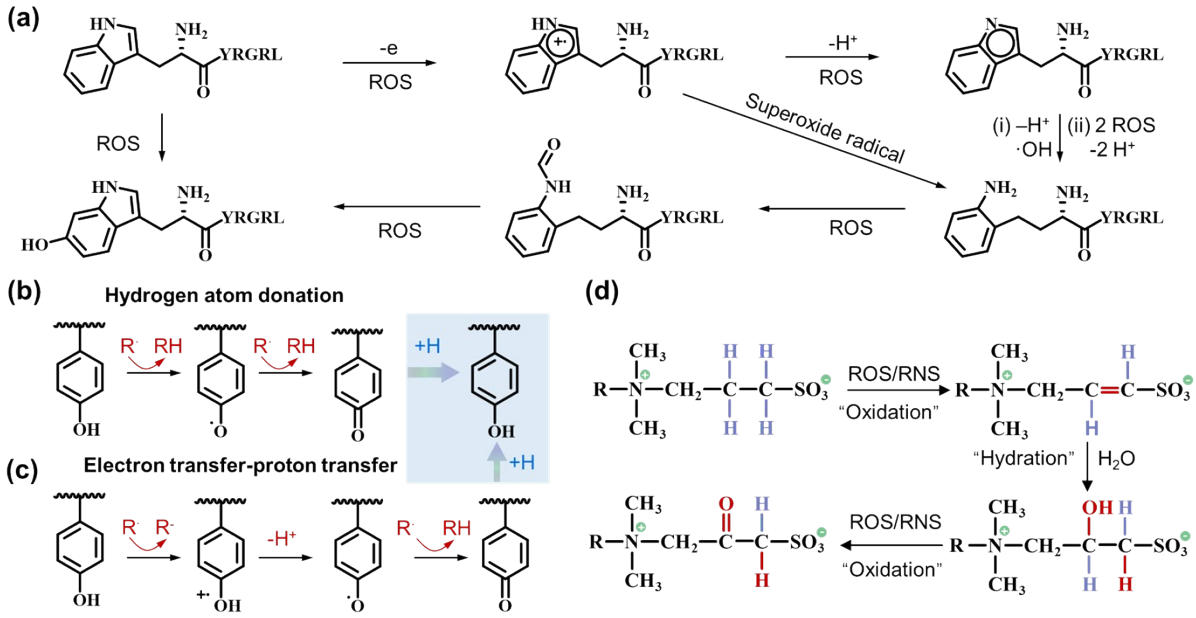

Scheme S4 The chemical mechanism of antioxidation of PSP.

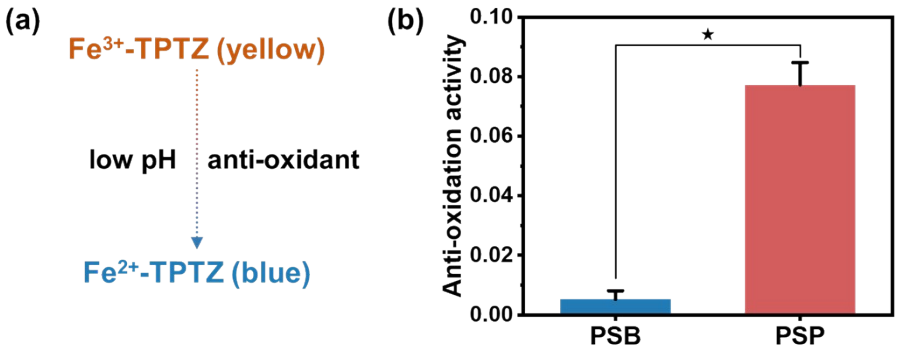

Figure S31 The total anti–oxidation activity of PSB and PSP at low pH. (a) anti–oxidation mechanism and (b) anti–oxidation activity. ★ ($p < 0.05$) implies statistical difference.

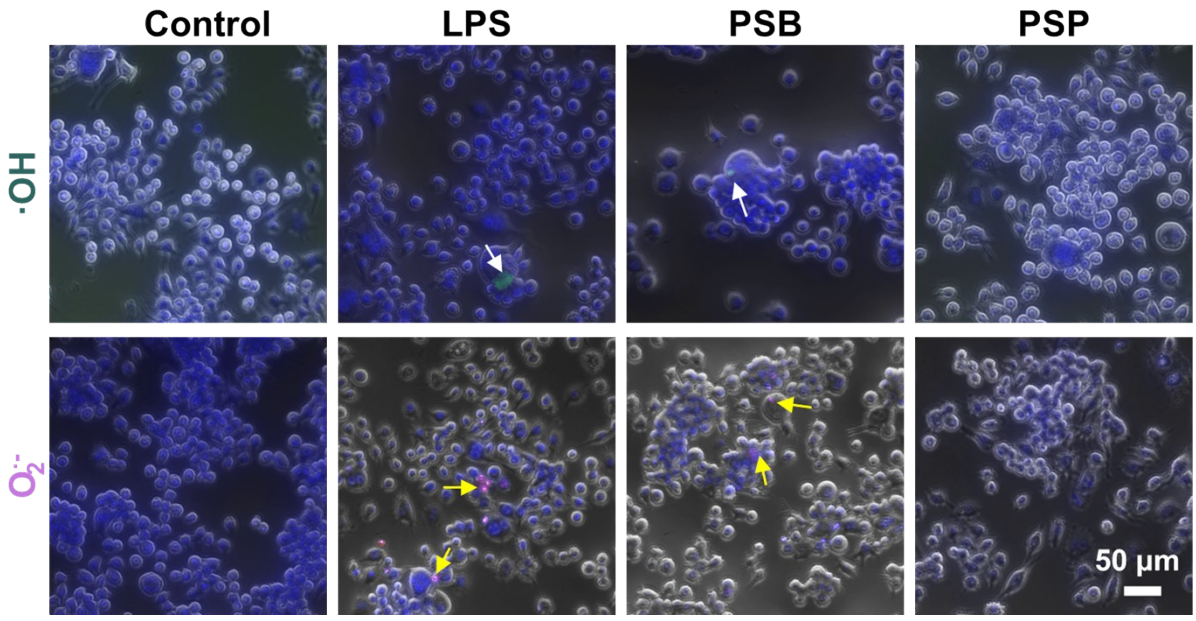

Figure S32 The ·OH and O·– 2 expressions of RAW264.7 cells in control, LPS, PSB and PSP groups. The white arrows represent ·OH radicals, and the yellow arrows indicate O·– 2 radicals.

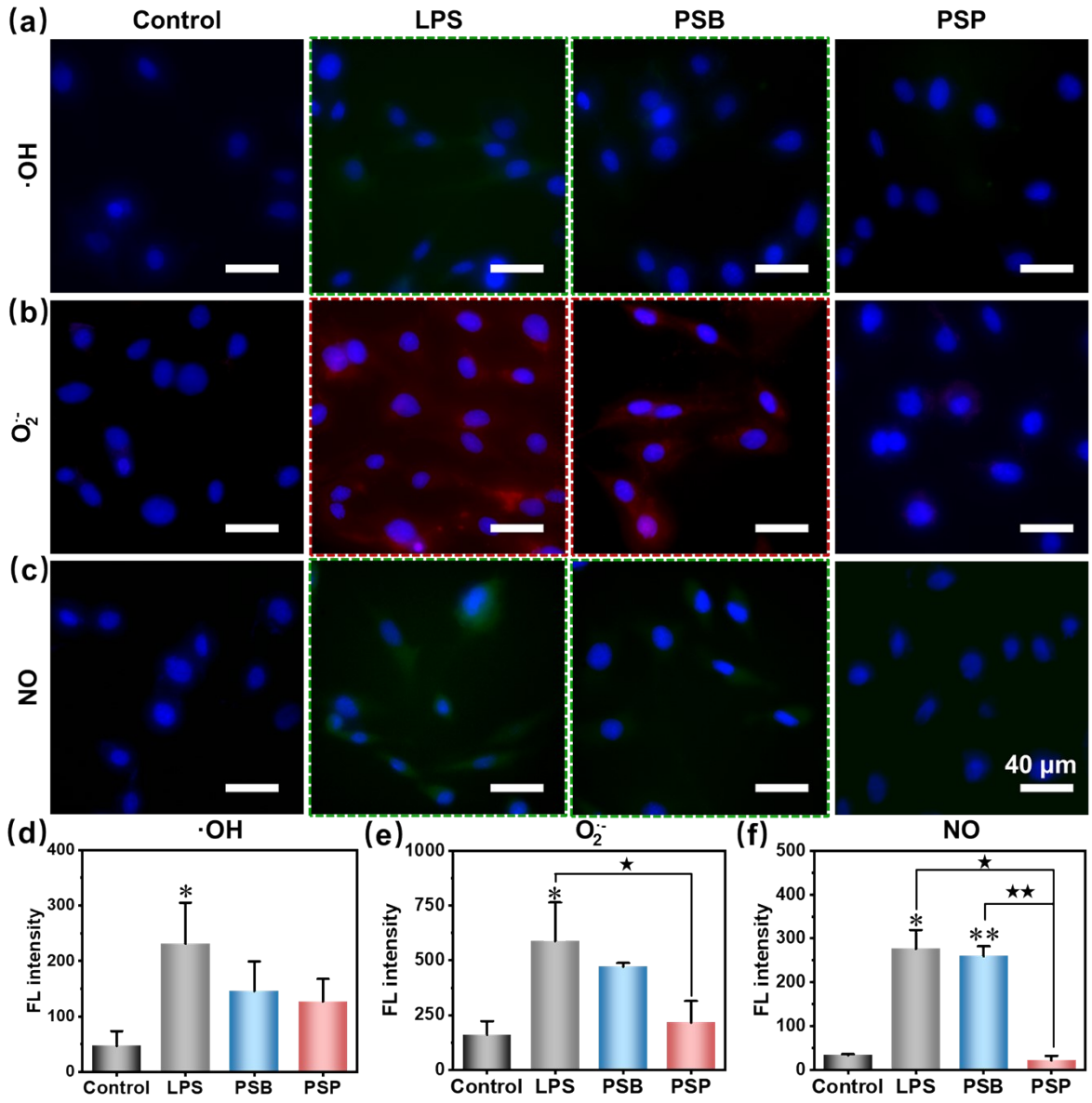

Figure S33 Anti–oxidation effect of PSP on chondrocytes stimulated by LPS. Intracellular (a) ·OH, (b) O·– 2 and (c) NO stained by DCFH–DA, DHE and DAF–FM dyes, respectively. (d–f) The corresponding fluorescence (FL) intensity to (a–c). * (p < 0.05) and ** (p <0.01) imply significant difference compared with the control group; ★ (p < 0.05) and ★★ (p <0.01) suggest statistical difference among other groups.

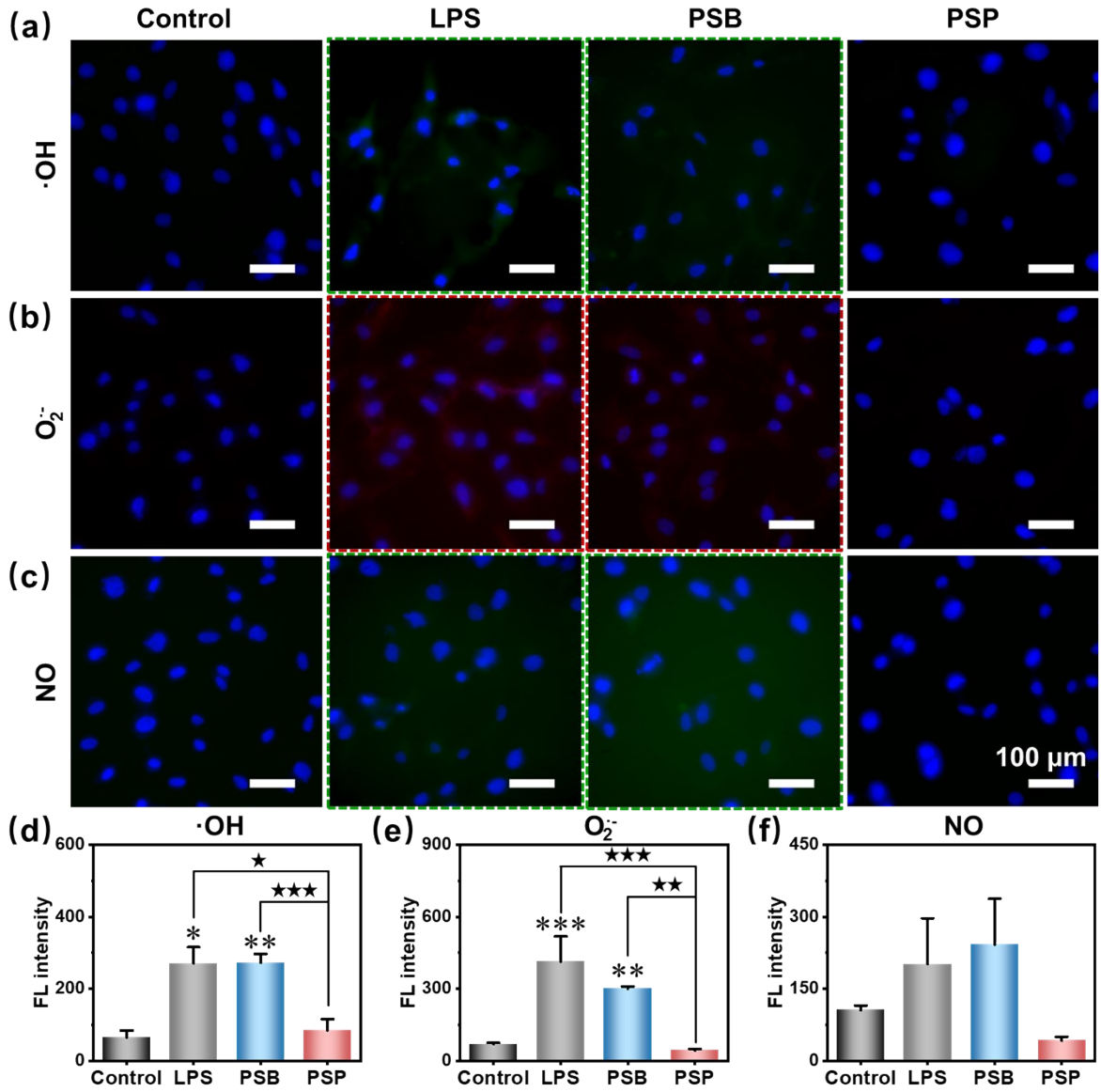

Figure S34 Anti–oxidation effect of PSP on SMSCs stimulated by LPS. Intracellular (a) ·OH, (b) O·– 2 and (c) NO stained by DCFH–DA, DHE and DAF–FM dyes, respectively. (d–f) The corresponding fluorescence (FL) intensity to (a–c). * ($p < 0.05$), ** ($p < 0.01$) and *** ($p < 0.001$) imply significant difference compared with the control group; ★ ($p < 0.05$), ★★ ($p < 0.01$) and ★★★ ($p < 0.001$) suggest statistical difference among other groups.

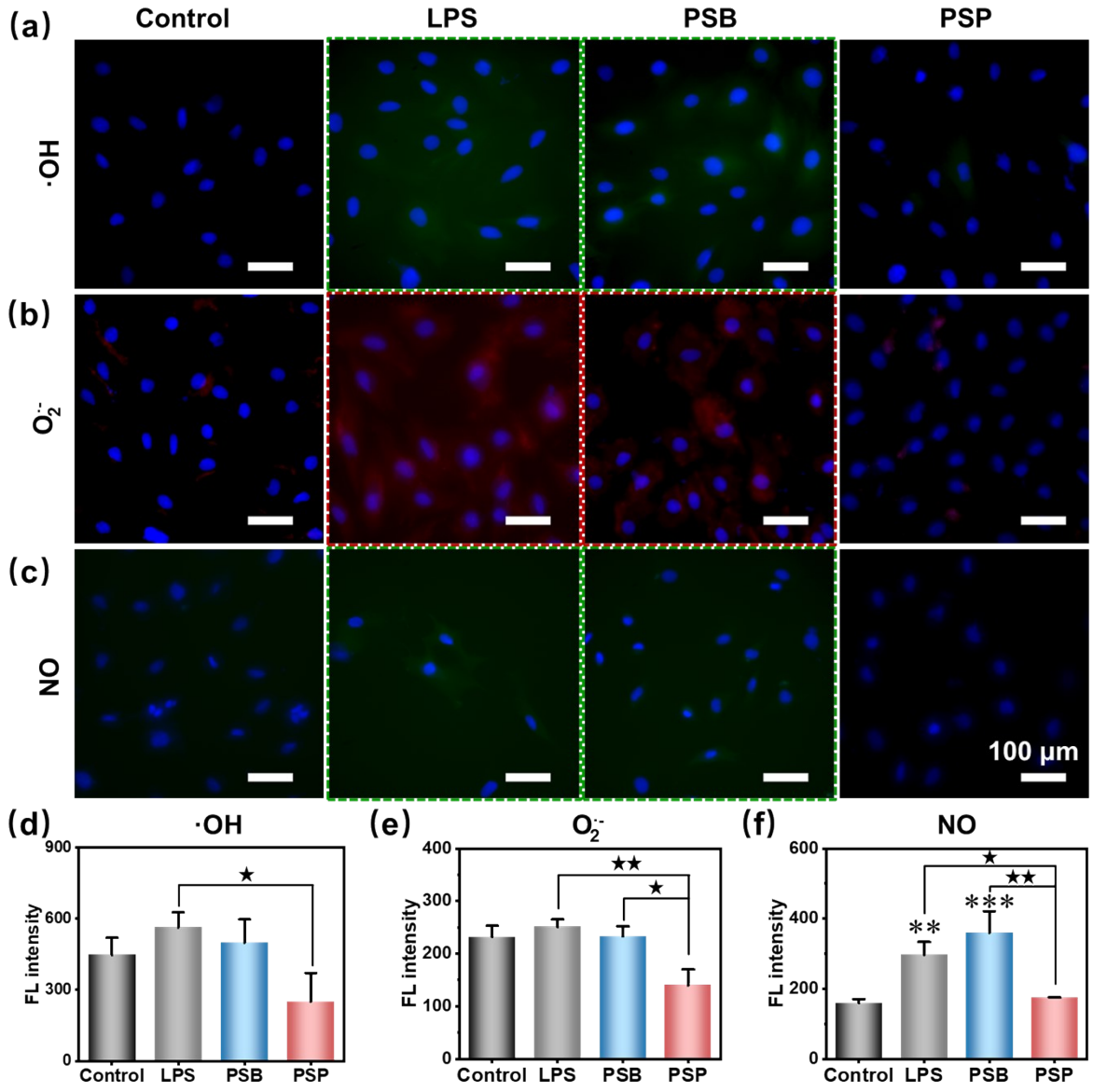

Figure S35 Anti–oxidation effect of PSP on BMSCs stimulated by LPS. Intracellular (a) ·OH, (b) O·– 2 and (c) NO stained by DCFH–DA, DHE and DAF–FM dyes, respectively. (d–f) The corresponding fluorescence (FL) intensity to (a–c). ** (p <0.01) and *** (p < 0.001) imply significant difference compared to the control group; ★ (p < 0.05) and ★★ (p < 0.01) suggest statistical difference among other groups.

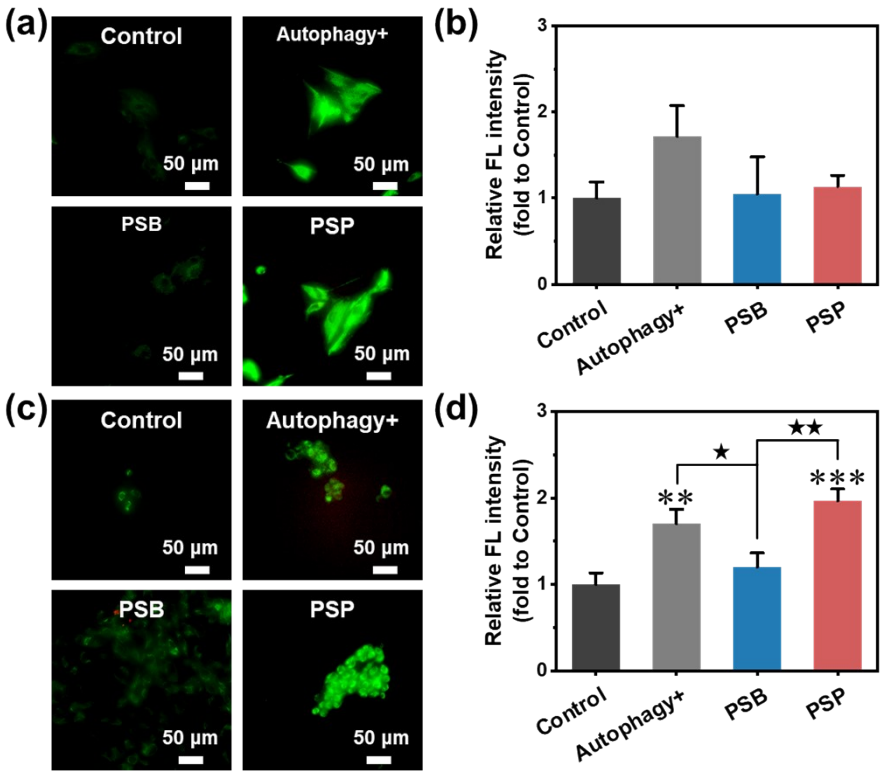

Figure S36 The activation of autophagy. (a) MDC/PI staining and (b) the relative fluorescence intensity of BMSCs. (c) MDC/PI staining and (d) the relative fluorescence intensity of SMSCs. The green color in (a) and (c) indicate cells with activated autophagy, and the red spots in (a) and (c) represent dead cells. ** ($p < 0.01$) and *** ($p < 0.001$) imply significant difference compared to the control group; ★ ($p < 0.05$) and ★★ ($p < 0.01$) suggest statistical difference among other groups.

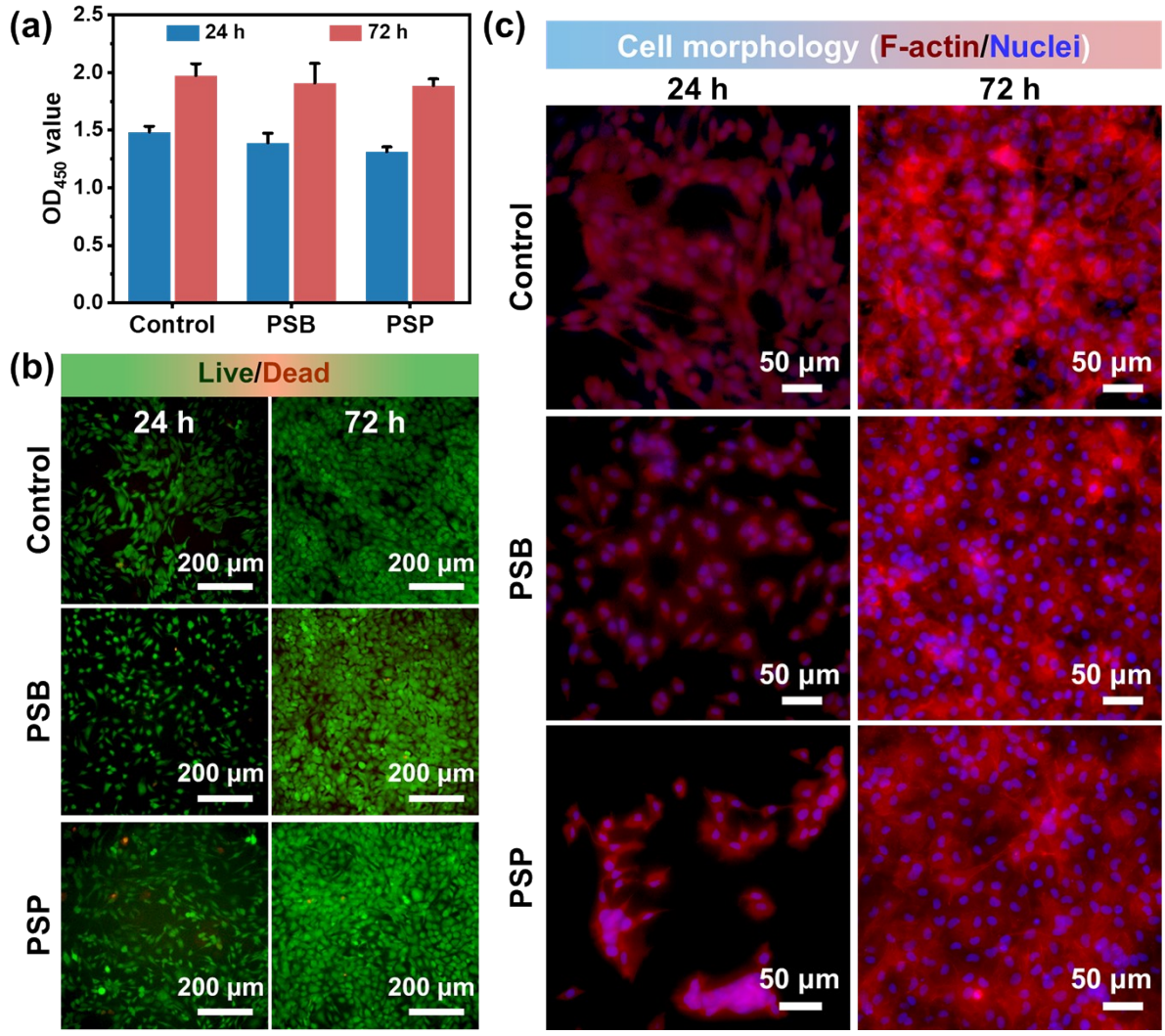

Figure S37 The cytocompatibility of PSB and PSP towards chondrocytes. (a) Cell proliferation, (b) live/dead staining images and (c) TRITC–phalloidin/DAPI staining images at 24 and 72 h. The green and red spots in (b) indicate live and dead cells, respectively. As for cell morphology, the nuclei were stained blue and the F–actin were stained red.

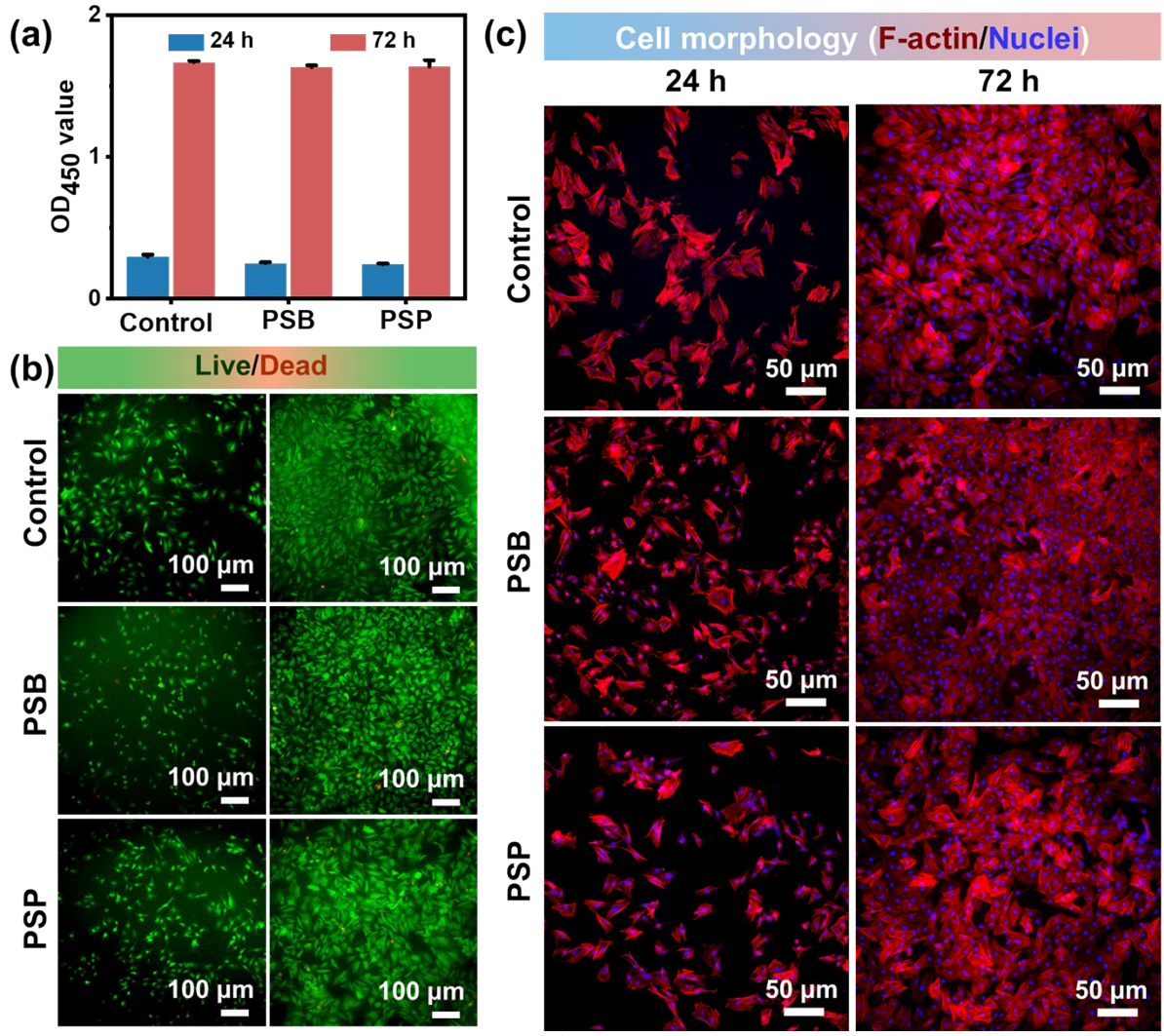

Figure S38 The cytocompatibility of PSB and PSP towards BMSCs. (a) Cell proliferation, (b) live/dead staining images and (c) TRITC–phalloidin/DAPI staining images at 24 and 72 h. The green and red spots in (b) indicate live and dead cells, respectively. As for cell morphology, the nuclei were stained blue and the F–actin were stained red.

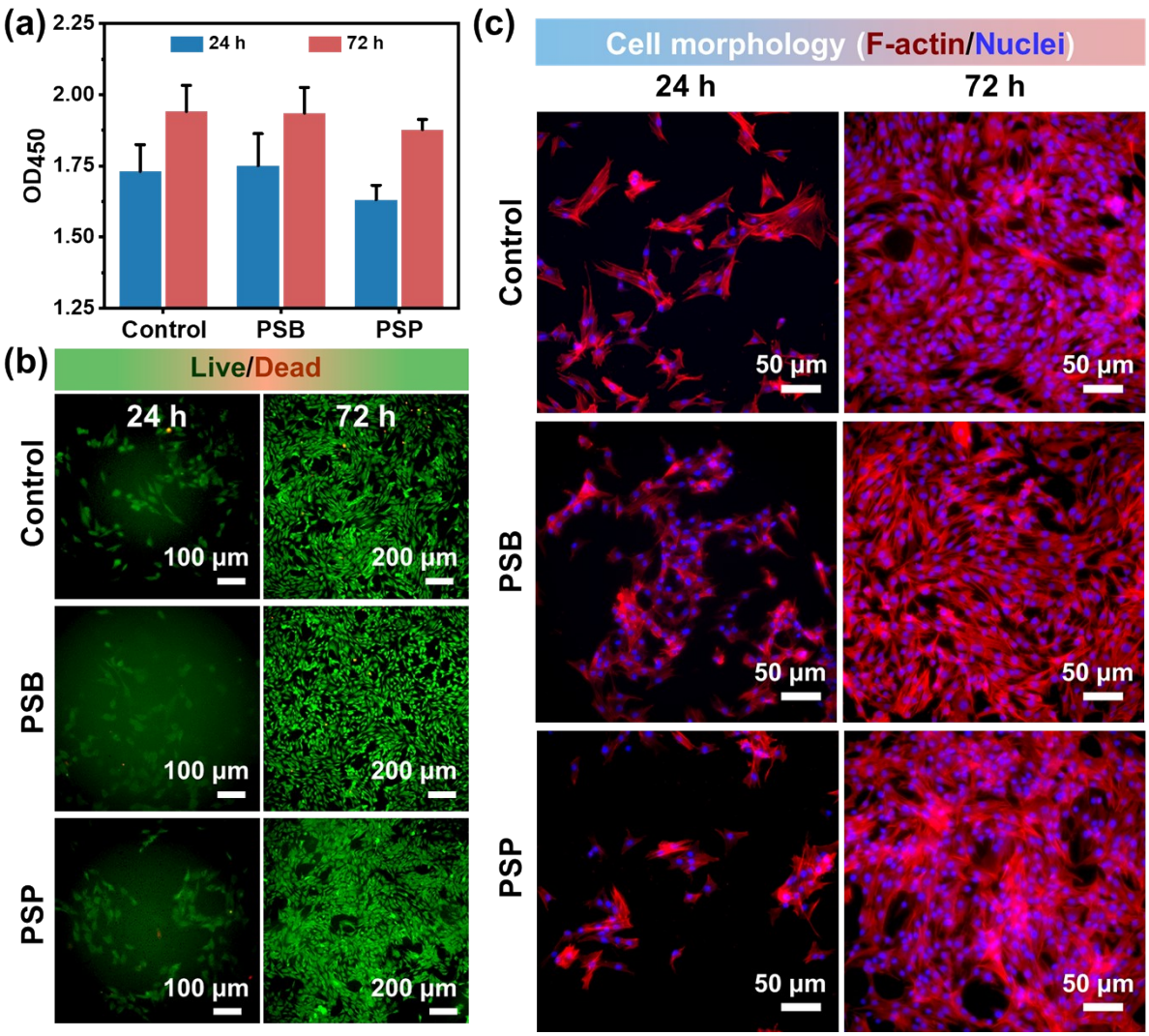

Figure S39 The cytocompatibility of PSB and PSP towards SMSCs. (a) Cell proliferation, (b) live/dead staining images and (c) TRITC–phalloidin/DAPI staining images at 24 and 72 h. The green and red spots in (b) indicate live and dead cells, respectively. As for cell morphology, the nuclei were stained blue and the F–actin were stained red.

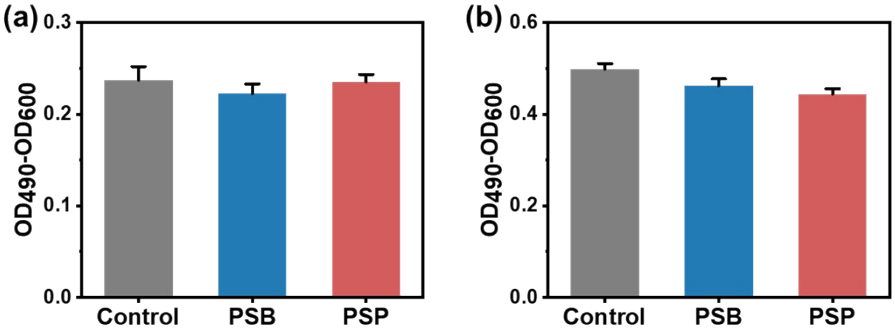

Figure S40 LDH release of (a) chondrocytes and (b) SMSCs incubated with PSB and PSP.

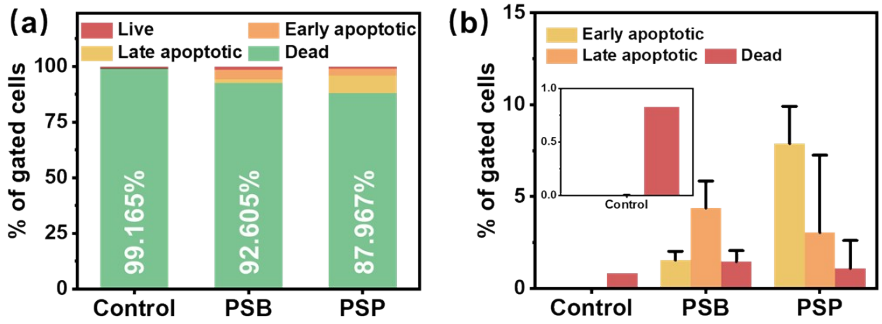

Figure S41 The flow cytometry analysis of chondrocytes incubated with PSB and PSP. (a) Percentage of live, early apoptotic, late apoptotic and dead cells, and (b) the quantitative illustration of percentage of apoptotic cells.

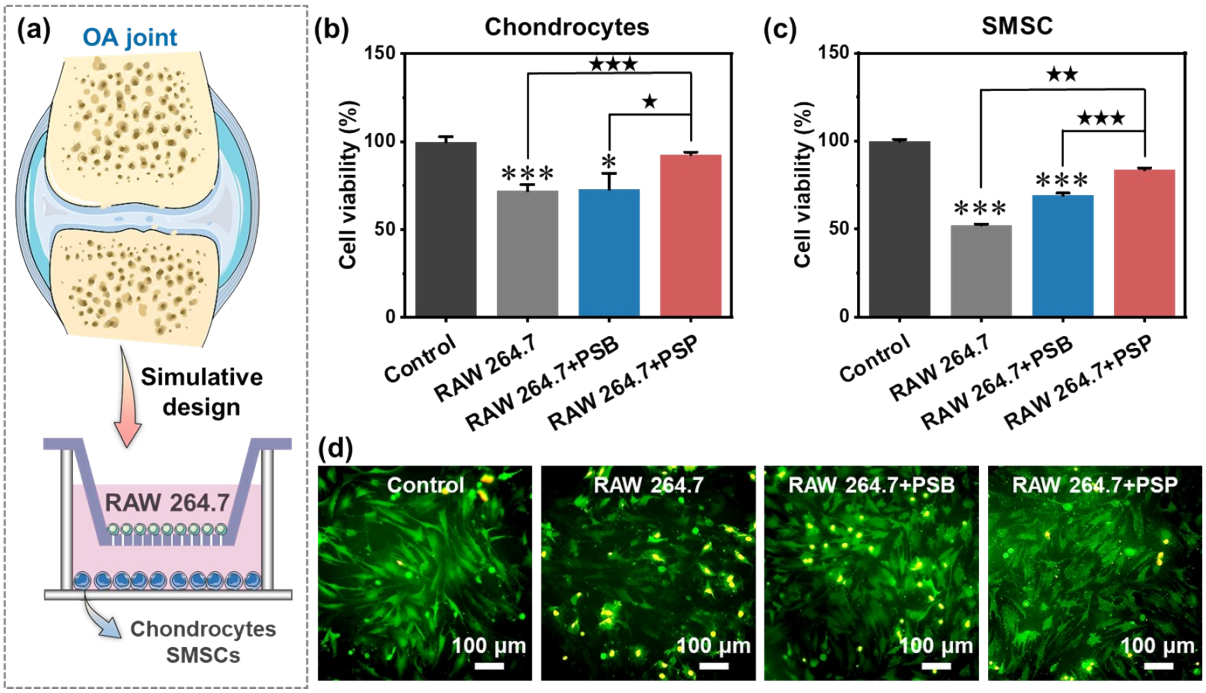

Figure S42 (a) Concept in designing co–culture system of RAW 264.7 cells and chondrocyte (or SMSCs) to evaluate the resistance of PSP towards inflammatory cells. The cell viability of (b) chondrocytes and (c) SMSCs when cocultured with RAW 264.7 cells in presence of PSP. (d) Live/Dead staining images of chondrocytes in the co–culture system. * ($p < 0.05$) and *** ($p < 0.001$) imply significant difference compared to the control group; ★ ($p < 0.05$), ★★ ($p < 0.01$) and ★★★ ($p < 0.001$) suggest statistical difference among other groups.

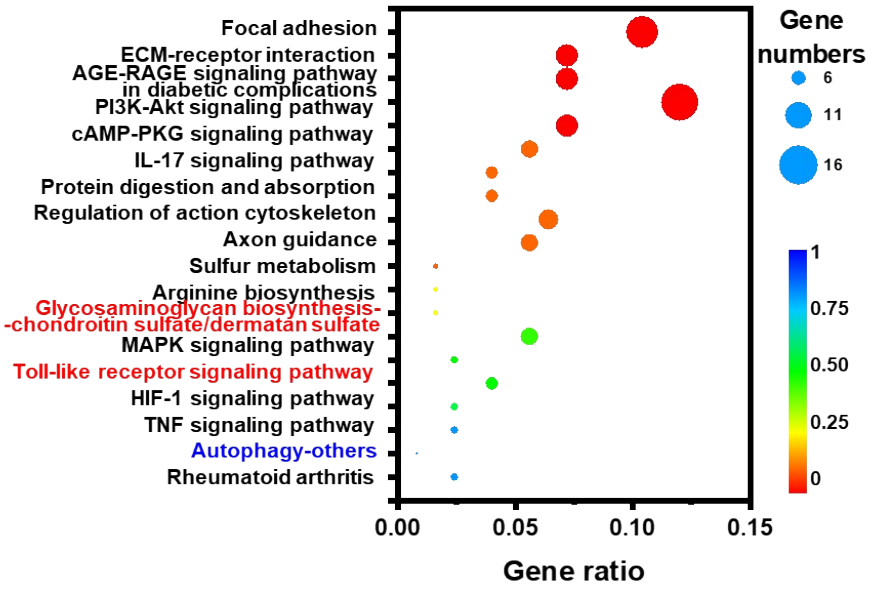

Figure S43 KEGG enrichment analysis of up–regulated DEGs.

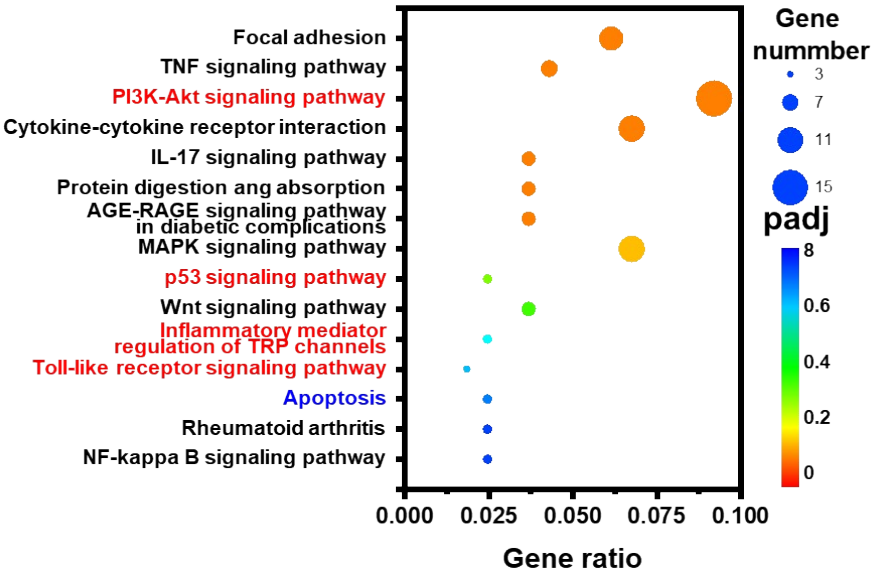

Figure S44 KEGG enrichment analysis of down–regulated DEGs.

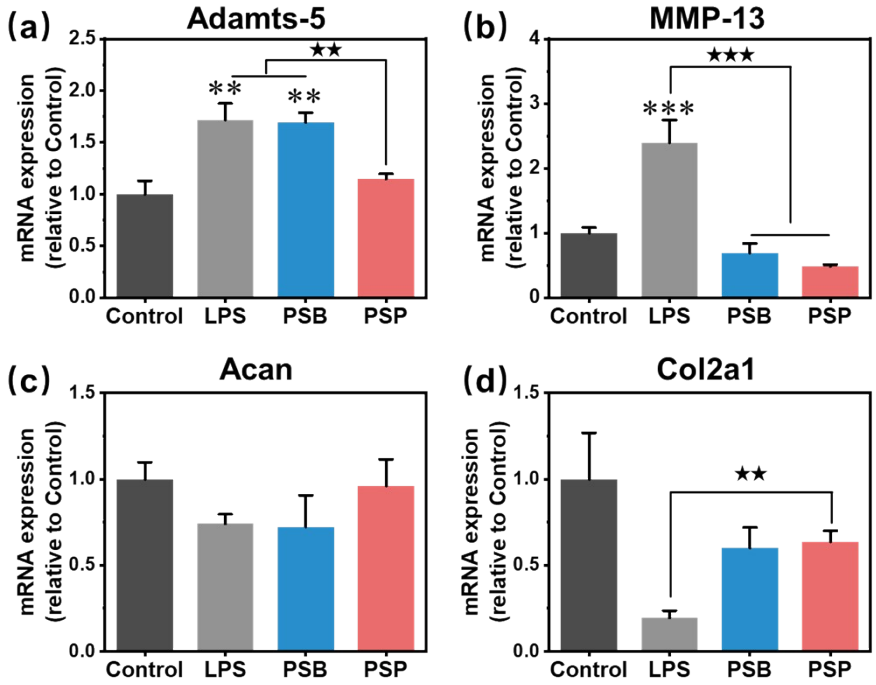

Figure S45 RT–aPCR analysis of LPS–stimulated chondrocytes incubated with PSB and PSP: (a) Adamts–5, (b) MMP–13, (c) Acan and (d) Col2a1. ** ($p < 0.01$) and *** ($p < 0.001$) is regarded as significant difference compared to control group, ★★ ($p < 0.01$) and ★★★ ($p < 0.001$) indicate statistical difference between other groups.

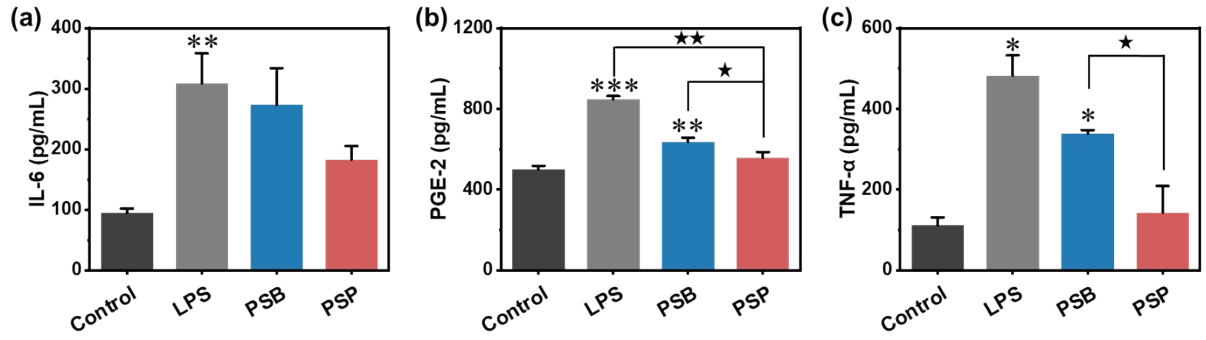

Figure S46 The expression of intracellular (a) IL–6, (b) PGE–2 and (c) TNF–α. * ($p < 0.05$), ** ($p < 0.01$) and *** ($p < 0.001$) is regarded as significant difference compared to control group, ★ ($p < 0.05$) and ★★ ($p < 0.01$) indicate statistical difference between other groups.

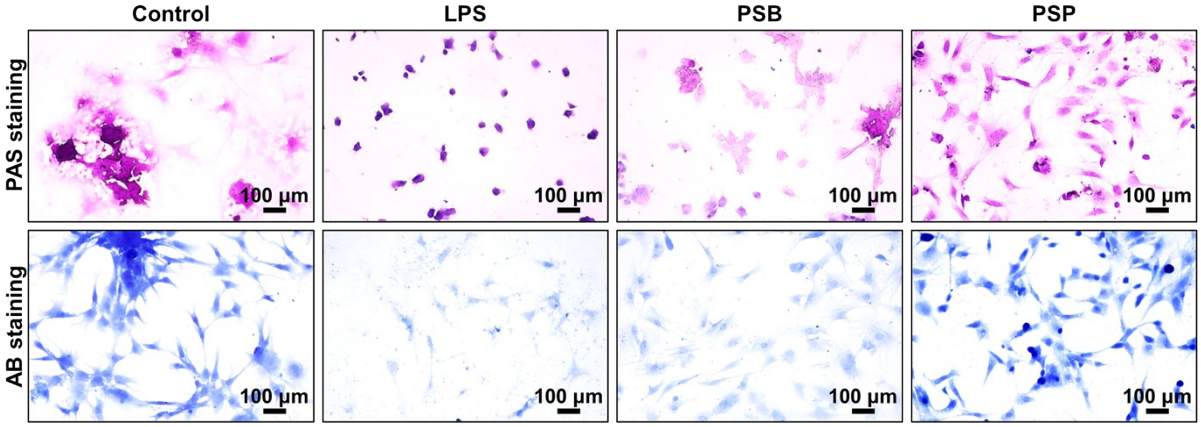

Figure S47 The PAS and SB staining images of control, LPS, PSB and PSP groups.

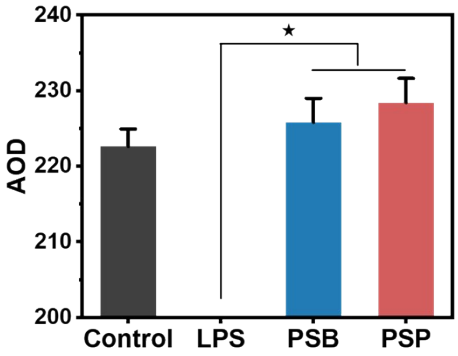

Figure S48 Semi–quantitative analysis of immunohistochemical staining of aggrecan. ★ ($p < 0.05$) indicates significant difference.

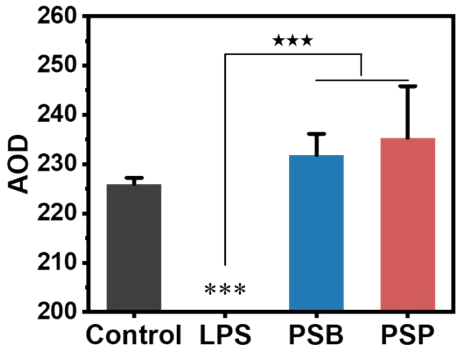

Figure S49 Semi–quantitative analysis of immunohistochemical staining of Col II. *** ($p < 0.001$) indicates significant difference compared to the control group, and ★★★ ($p < 0.001$) implies the statistical difference among other groups.

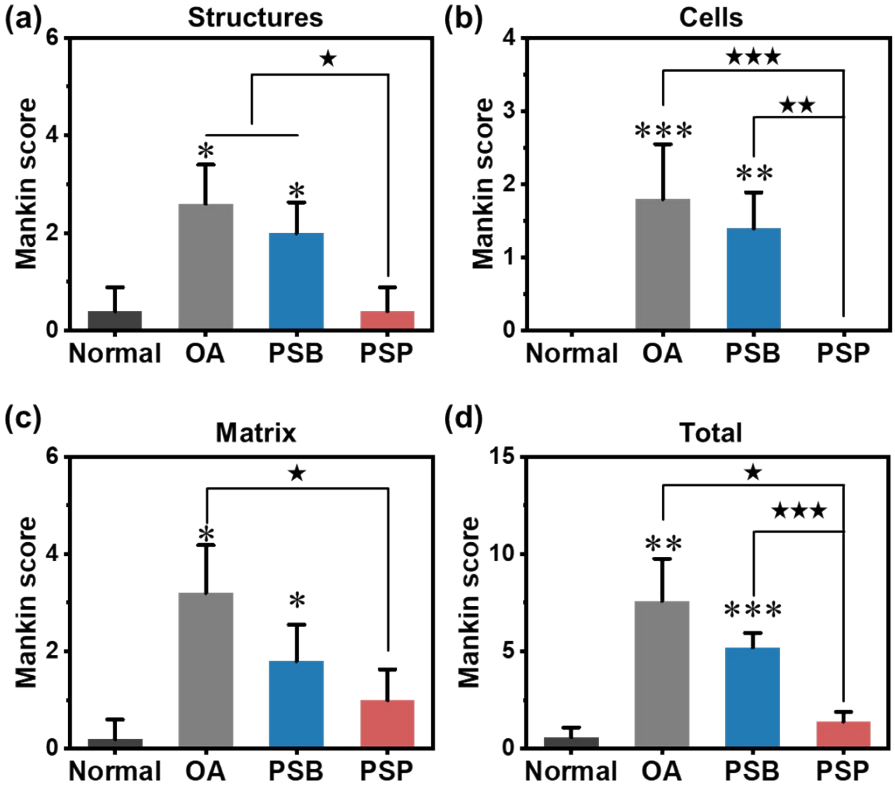

Figure S50 Mankin score of normal, OA, PSB and PSP groups: (a) structures, (b) cells, (c) matrix and (d) total scores. * ($p < 0.05$), ** ($p < 0.01$) and *** ($p < 0.001$) is regarded as significant difference compared to control group, ★ ($p < 0.05$), ★★ ($p < 0.01$) and ★★★ ($p < 0.001$) indicate statistical difference between other groups.

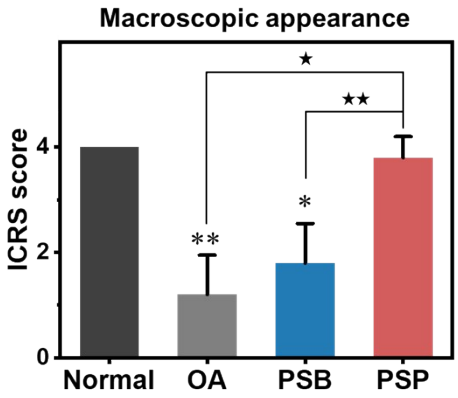

Figure S51 ICRS score (macroscopic appearance) of normal, OA, PSB and PSP group. * ($p < 0.05$) and ** ($p < 0.01$) is regarded as significant difference compared to control group, ★ ($p < 0.05$) and ★★ ($p < 0.01$) indicate statistical difference between other groups.

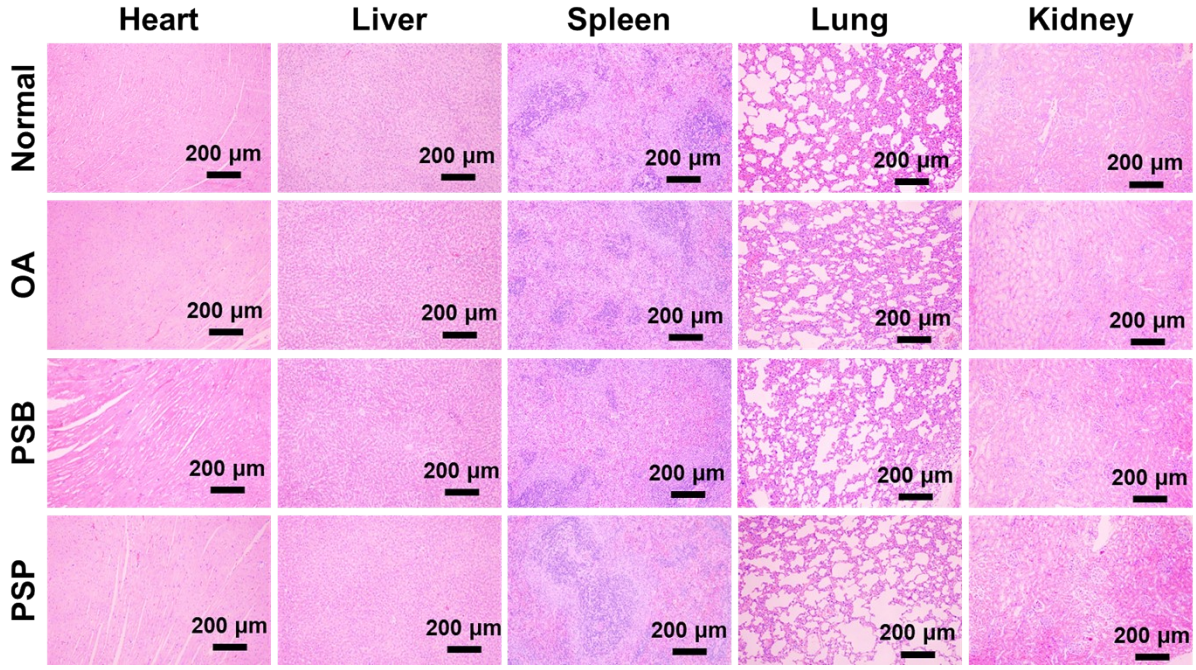

Figure S52 H&E staining slices of major organs (heart, liver, spleen, lung and kidney) of SD rats from normal, OA, PSB and PSP groups.

S4. Supplementary Tables

Table S1 Chemical composition of PSB, PSN and PSP from XPS analysis.

	C (%)	N (%)	O (%)	S (%)
PSB	63.36	5.74	25.5	5.4
PSN	64.29	5.92	24.57	5.21
PSP	62.78	6.61	25.51	5.09

Table S2 Biosafety parameters analyzed by blood routine examination

	Normal	OA	PSB	PSP
Gran# ($\times10^9$/L)	0.52 ± 0.12	0.42 ± 0.10	0.46 ± 0.08	0.48 ± 0.21
WBC ($\times10^9$/L)	2.15 ± 0.25	2.2 ± 0.19	1.88 ± 0.08	2.36 ± 0.41
Lymph# ($\times10^9$/L)	1.68 ± 0.29	1.75 ± 0.15	1.26 ± 0.16	1.7– ± 0.13
Mon# ($\times10^9$/L)	0.10 ± 0.00	0.1– ± 0.00	0.10 ± 0.10	0.10 ± 0.06
Gran%	23.58 ± 3.61	18.73 ± 2.40	23.45 ± 4.26	20.64 ± 7.08
Lymph%	71.94 ± 3.80	77.70 ± 2.90	69.64 ± 6.31	75.04 ± 8.21
Mon%	4.48 ± 0.47	4.36 ± 0.69	4.55 ± 0.47	4.26 ± 1.15
RBC ($\times10^{12}$/L)	7.81 ± 0.17	8.03 ± 0.25	7.96 ± 0.23	7.70 ± 0.28
HGB (g/L)	155.40 ± 5.61	154.00 ± 3.85	150.80 ± 4.71	149.80 ± 3.54
MCHC (g/L)	339.40 ± 5.61	334.80 ± 2.23	332.80 ± 4.07	333.40 ± 2.58
PLT ($\times10^9$/L)	1024.60 ± 198.85	1028.75 ± 32.34	1212.00 ± 155.04	1116.00 ± 162.23
PDW	16.72 ± 0.13	16.72 ± 0.17	16.54 ± 0.16	16.60 ± 0.26
HCT (%)	45.70 ± 1.63	45.94 ± 3.84	45.28 ± 1.78	44.88 ± 0.82
MCV (fL)	58.56 ± 1.65	57.30 ± 1.96	56.92 ± 1.84	58.38 ± 1.76
MCH (pg)	19.84 ± 0.74	19.14 ± 0.65	18.86 ± 0.49	19.40 ± 0.49
RDW (%)	12.38 ± 0.54	12.30 ± 0.88	12.52 ± 1.08	12.02 ± 0.40
MPV (fL)	6.52 ± 0.27	6.36 ± 0.21	6.28 ± 0.27	6.24 ± 0.50

Gran#, granulocyte; WBC, white blood cell count; Lymph#, lymphocyte count; Mon#, monocyte count; Gran%, percentage of granulocyte; Lymph%, percentage of lymphocyte; Mon%, percentage of monocyte; RBC, red blood cell count; HGB, hemoglobin; MCHC, mean corpuscular hemoglobin concentration; PLT, platytroctid; PDW, platelet distribution width; HCT, hematocrit; MCV, mean corpuscular volume; MCH, mean corpuscular hemoglobin; RDW, red blood cell volume distribution width; MPC, mean platelet volume.

Table S3 Primer sequences for RT–qPCR

Target gene	Forward primer sequence	Reverse primer sequence
ACTB	GAAGATCAAGATCATTGCTCCT	TACTCCTGCTTGCTGATCCACA
Adamts–5	GCAGAACATCGACCAACTCTACTC	CCAGCAATGCCCACCGAAC
MMP 13	GGTGATGAAGATGATTTGTCTGAGG	CGTCAAGTTTGCCAGTCACCT
Acan	CTGAACGACAGGACCATCGAA	CGTGCCAGATCATCACCACA
Col2a1	CACTCAAGTCCCTCAACAACCAG	GGGGTCAATCCAGTAGTCTCCAC

Tables S4 The OA therapeutic effect of various polymeric biomaterials

Polymeric biomaterials	Drugs	Score reduction [a]	Number [b]	Ref.
MSNs–NH_2@PMPC	–	4.64	A1	9
	+DS	30.55	D1	
PEG–PPG–PEG	–	5.74	A2	10
	+ASTA	50.76	D5	
PEG–PTK–PEG	–	66.02	A19	
	+ASTA	75.79	D13	
MSNs–NH_2@PSPMK	–	6.60	A3	3
	+DS	35.38	D3	
MHS	–	8.90	A4	11
	+PPKHF	71.77	D11	
MSNs	–	11.00	A5	9
	–	19.15	A8	3
HA@MPC	–	17.96	A6	12
	+DS	62.80	D9	
MMSP	–	18.61	A7	13
	+DS	55.13	D7	
TPP–MMSP	–	39.20	A13	
	+DS	79.30	D15	
GelMA@DMA–MPC	–	23.73	A9	14
	+DS	31.92	D2	
PMS	–	24.70	A10	15
	+NF	59.59	D8	
BB	–	25.34	A11	16
	+Cur & LXP	71.80	D12	
CB	–	60.03	A17	
	+Cur & LXP	87.52	D17	
PMPC–Lipo	–	31.18	A12	17
	+GA	64.69	D10	
8–arm PEG–COLBP	–	41.61	A14	18
HABP2–8–arm PEG–ColBP	–	46.49	A16	
–	Orthovisc	22.45	B1	
P(DMA–b–SBMA)	–	42.52	A15	19
HA–MPC	–	64.99	A18	20
PTKU	–	72.31	A20	21
	+DEX	86.82	D16	
–	HA	25.19	B2	12
		40.03	B3	20
		59.57	B4	22
–	PSO	14.63	C1	23
	DS	23.31	C2	24
	ASTA	31.12	C3	10
	NF	45.13	C4	15
	DEX	50.09	C5	21
MR–PPL	+PSO	46.97273891	D4	23
MRC–PPL		79.1117236	D14	
MoS_2–PDMPC	+DS	51.26292212	D6	24
PSB–*b*–PColBP	–	76	This work	

[a] Score reduction is chosen to evaluate the therapeutic effect on OA, which is calculated by the reduced ratio of OARSI scores in comparison to the control (or normal) group.

[b] The number is linked with the heat map in Fig. 6f in the main text.

S5. References

1. W. Peng, P. Liu, X. Zhang, J. Peng, Y. Gu, X. Dong, Z. Ma, P. Liu and J. Shen, *Chem. Eng. J.*, 2020, **398**, 125663.
2. P. Yu, Y. Li, H. Sun, X. Ke, J. Xing, Y. Zhao, X. Xu, M. Qin, J. Xie and J. Li, *ACS Appl. Mater. Interfaces*, 2022, **14**, 27360-27370.
3. Y. Yan, T. Sun, H. Zhang, X. Ji, Y. Sun, X. Zhao, L. Deng, J. Qi, W. Cui, H. A. Santos and H. Zhang, *Adv. Funct. Mater.*, 2019, **29**, 1807559.
4. A. Singh, M. Corvelli, S. A. Unterman, K. A. Wepasnick, P. McDonnell and J. H. Elisseeff, *Nat. Mater.*, 2014, **13**, 988-995.
5. P. Yu, J. Xie, Y. Chen, J. Liu, Y. Liu, B. Bi, J. Luo, S. Li, X. Jiang and J. Li, *J. Mater. Chem. B*, 2020, **8**, 270-281.
6. Yihan Liao, Yinshi Ren, Xin Luo, Anthony J. Mirando, Jason T. Long, Abigail Leinroth, Ru-Rong Ji and M. J. Hilton, *Sci. Signal.*, 2022, **15**, eabn7082.
7. Y. Jin, Q. Liu, P. Chen, S. Zhao, W. Jiang, F. Wang, P. Li, Y. Zhang, W. Lu, T. P. Zhong, X. Ma, X. Wang, A. Gartland, N. Wang, K. M. Shah, H. Zhang, X. Cao, L. Yang, M. Liu and J. Luo, *Cell Discov.*, 2022, **8**, 24.
8. G. Yang, M. Fan, J. Zhu, C. Ling, L. Wu, X. Zhang, M. Zhang, J. Li, Q. Yao, Z. Gu and X. Cai, *Biomaterials*, 2020, **255**, 120155.
9. H. Chen, T. Sun, Y. Yan, X. Ji, Y. Sun, X. Zhao, J. Qi, W. Cui, L. Deng and H. Zhang, *Biomaterials*, 2020, **242**, 119931.
10. H. Xiong, S. Wang, Z. Sun, J. Li, H. Zhang, W. Liu, J. Ruan, S. Chen, C. Gao and C. Fan, *Appl. Mater. Today*, 2022, **26**, 101366.
11. Y. Yao, G. Wei, L. Deng and W. Cui, *Adv. Sci.*, 2023, **10**, 2207438.
12. L. Yang, L. Sun, H. Zhang, F. Bian and Y. Zhao, *ACS Nano*, 2021, **15**, 20600-20606.
13. L. Zhang, X. Chen, P. Cai, H. Sun, S. Shen, B. Guo and Q. Jiang, *Adv. Mater.*, 2022, **34**, 2202715.
14. Y. Han, J. Yang, W. Zhao, H. Wang, Y. Sun, Y. Chen, J. Luo, L. Deng, X. Xu, W. Cui and H. Zhang, *Bioac. Mater.*, 2021, **6**, 3596-3607.
15. Z. Han, L. Bai, J. Zhou, Y. Qian, Y. Tang, Q. Han, X. Zhang, M. Zhang, X. Yang, W. Cui and Y. Hao, *Biomaterials*, 2022, **285**, 121545.
16. M. Zhang, X. Peng, Y. Ding, X. Ke, K. Ren, Q. Xin, M. Qin, J. Xie and J. Li, *Mater. Horizons*, 2023, **10**, 2554-2567.
17. H. Yang, R. Yan, Q. Chen, Y. Wang, X. Zhong, S. Liu, R. Xie and L. Ren, *J. Colloid Interface Sci.*, 2023, **652**, 2167-2179.

18. H. J. Faust, S. D. Sommerfeld, S. Rathod, A. Rittenbach, S. Ray Banerjee, B. M. W. Tsui, M. Pomper, M. L. Amzel, A. Singh and J. H. Elisseeff, *Biomaterials*, 2018, **183**, 93-101.
19. W. Zhao, Y. Yu, Z. Zhang, D. He and H. Zhang, *ACS Appl. Mater. Interfaces*, 2022, **14**, 35409-35422.
20. Y. Zheng, Y. Yan, W. Zhao, H. Wang, Y. Sun, J. Han and H. Zhang, *ACS Appl. Mater. Interfaces*, 2022, **14**, 21773-21786.
21. H. Zhang, H. Xiong, W. Ahmed, Y. Yao, S. Wang, C. Fan and C. Gao, *Chem. Eng. J.*, 2021, **409**, 128147.
22. R. Xie, H. Yao, A. S. Mao, Y. Zhu, D. Qi, Y. Jia, M. Gao, Y. Chen, L. Wang, D. A. Wang, K. Wang, S. Liu, L. Ren and C. Mao, *Nat. Biomed. Eng.*, 2021, **5**, 1189-1201.
23. Q. Lan, R. Lu, H. Chen, Y. Pang, F. Xiong, C. Shen, Z. Qin, L. Zheng, G. Xu and J. Zhao, *J. Nanobiotech.*, 2020, **18**, 117.
24. W. Qiu, W. Zhao, L. Zhang, H. Wang, N. Li, K. Chen, H. Zhang and Y. Wang, *Adv. Funct. Mater.*, 2022, **32**, 2208189.